Space Science Reviews (2026) 222:42
https://doi.org/10.1007/s11214-026-01301-x

Stellar Astrophysics in the Ultraviolet: Setting the Scene

Xiaoting Fu[1] · Giulio Del Zanna[2,3] · Li Ji[1] · Stephan Geier[4] · Matti Dorsch[4] · Vikrant Jadhav[5,6] · Firoza Sutaria[7] · Chengyuan Li[8,9] · Quentin Parker[10] · Xuan Fang[11,12]

Received: 2 December 2025 / Accepted: 20 April 2026
© The Author(s) 2026

Abstract
The ultraviolet (UV) spectral domain occupies a unique position in stellar astrophysics, serving as the bridge between the thermal continuum of photospheres and the high-energy, non-thermal processes of stellar coronae and winds. This article provides a review of stellar physics in the UV, addressing both the theoretical framework and observational applications across the Hertzsprung-Russell diagram. We explicitly structure our discussion around key scientific questions, demonstrating that accurate spectral synthesis in this regime demands Non-LTE radiative transfer codes, which in turn rely on precise atomic collision and recombination rates. We highlight how a critical scarcity of modern laboratory astrophysics data limits these models, particularly for complex ions. Moving to observational diagnostics, we review how UV spectroscopy constrains diffusion and radiatively driven winds in hot subluminous stars, and traces shock dynamics and abundance patterns in Planetary Nebulae and Supernova Remnants. In the context of star clusters, we illustrate how UV sensitivity to light-element variations (C, N, O) allows us to disentangle multiple stellar populations that appear degenerate in optical bands. We conclude that future progress depends on facilities capable of high-resolution spectroscopy, time-domain monitoring, and polarimetry to recover these diagnostic tracers and resolve the physics of stellar feedback.

Keywords Ultraviolet · Star · Model atmosphere · Star cluster

1 Stellar Astrophysics in UV: Scientific Questions

The Ultraviolet (UV) regime occupies a critical "middle ground" in the electromagnetic spectrum, bridging the gap between the thermal continuum of the optical window and the high-energy, non-thermal processes dominated by X-rays. Spanning the wavelength range roughly from the Lyman limit ($\sim$ 912 Å) up to the atmospheric cutoff ($\sim$ 3200 Å or 4000 Å, depending on definition). The UV band corresponds to energy transitions of a few electron volts (eV). This is the energy scale that high enough to excite or ionize many atoms and molecules. Thus the UV maps where material is, as all bands do, while also offering particularly direct constraints on its ionization and excitation state through abundant resonance lines and photoionization thresholds.

We further subdivide the UV range into near-UV (NUV; $\sim$2000–4000 Å), far-UV (FUV; $\sim$912–2000 Å), and sometimes extreme-UV (EUV; $\lesssim$ 912 Å). The precise numerical boundaries are conventional, but the subdivisions track distinct physical regimes. While NUV

Extended author information available on the last page of the article

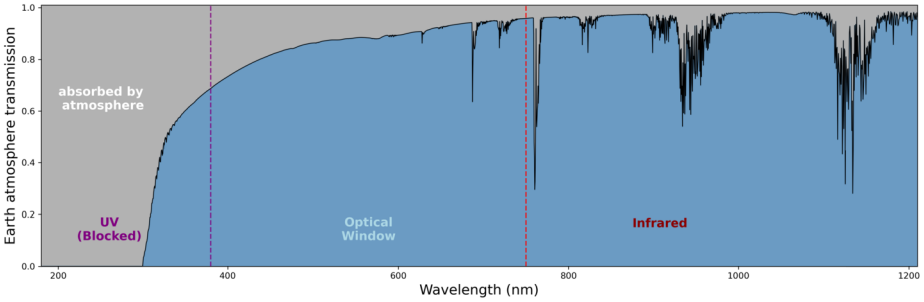

Fig. 1 The Earth atmosphere transmission curve in UV, optical, and near infrared. Most of the flux in UV wavelength is absorbed by the Earth atmosphere. The vertical purple and red dashed lines illustrate the wavelength separation

photons mostly probe photospheric continua and relatively low-ionization lines, FUV and EUV emission requires much higher energies, predominantly revealing hot, tenuous plasmas (coronae, shocked winds, hot white dwarfs, AGN accretion disks). Because these high-energy photons are highly effective at ionizing and dissociating molecules, their absorption governs the physical and chemical state of the surrounding gaseous environment. The UV band therefore provides a direct link between stellar atmospheric physics, mass loss, and the radiative feedback that shapes the surrounding gas.

According to Wien's Law, the Planck function for hot stars (O and B types massive stars, as well as White Dwarfs) peaks directly in the UV. Even for solar-type stars that peak in the optical, the UV provides a unique probe of stellar activity (Ayres et al. 1981; Noyes et al. 1984). Chromospheric and coronal emissions, indicative of magnetic heating and flares, are best traced in the UV. The UV spectrum is also densely packed with resonance lines of abundant metallic ions (e.g., C IV, Mg II, Si IV). These lines are incredibly sensitive diagnostics of stellar atmospheres, allowing us to measure mass-loss rates (Morton 1967; Puls et al. 2008; Walborn and Panek 1984), accretion flows in young stellar objects (YSOs) (Calvet and Gullbring 1998), and the interaction between stars and their circumstellar environments. Beyond the surface of the star, ultraviolet radiation acts as the primary currency of energy exchange in the interstellar medium (ISM). UV photons are responsible for photoionizing hydrogen and metals in H II regions (Osterbrock and Ferland 2006), powering photodissociation regions (PDRs) on molecular-cloud surfaces (Haardt and Madau 1996, 2012; Hollenbach and Tielens 1999), and governing much of the heating and chemistry of the diffuse interstellar and circumgalactic medium (Tumlinson et al. 2017).

Through these mechanisms, the UV output of massive stars creates a feedback loop that regulates star formation efficiency and drives the phase structure of the galactic environment. Without understanding the UV radiation field, we cannot accurately model the chemical enrichment or the thermodynamic state of the gas from which future generations of stars will be born.

Despite its diagnostic power, UV astronomy is intrinsically challenging because the Earth's atmosphere is largely opaque at these wavelengths.

Unlike optical wavelength window, which can be observed freely from the ground because the Earth atmosphere is almost transparent to it, UV radiation is mostly absorbed by the atmosphere. This situation is illustrated in Fig. 1,[1] which shows the transmission of the

[1]The Earth atmosphere transmission curve is calculated with the ESO SKYCALC Sky Model Calculator (https://www.eso.org/observing/etc/bin/gen/form?INS.MODE=swspectr+INS.NAME=SKYCALC). The

Earth's atmosphere as a function of wavelength. The atmospheric transmission drops precipitously below ~ 4000 Å. Only a narrow NUV window at the very long wavelength end of UV can be accessed from high-altitude ground-based observatories, and even there atmospheric extinction and airglow are severe. This "UV Barrier", produced mainly by absorption in ozone (O_3) and molecular oxygen (O_2), strongly attenuates solar and astrophysical UV at the surface. It reduces biologically damaging UV fluxes for modern surface ecosystems while simultaneously preventing ground-based astronomy from accessing most of the cosmic UV spectrum.

For decades, this absorption meant that the UV universe remained a theoretical abstraction. It was not until the dawn of the space age that we could lift the curtain. Essentially all astrophysically useful UV spectroscopy and deep imaging must be carried out from above the atmosphere, using sounding rockets, balloons, satellites or instruments on platforms such as the Hubble Space Telescope (HST). Over the past few decades, a small number of dedicated missions have defined the field: the International Ultraviolet Explorer (IUE; Boggess et al. 1978), the Far Ultraviolet Spectroscopic Explorer (FUSE; Moos et al. 2000), the Extreme Ultraviolet Explorer (EUVE; Bowyer and Malina 1991), GALEX (Martin et al. 2005), and HST's UV instruments e.g. STIS (Woodgate et al. 1998), COS (Green et al. 2012), GGRS (Brandt et al. 1994), FOS (Harms and Fitch 1991) and ACS (Ford et al. 2003) among them. These missions have produced rich archival datasets, but their lifetimes, sky coverage, and instrument capabilities are limited compared to the vast diversity of optical and infrared facilities.

The importance of the UV extends far beyond the study of local stellar environments. It has become the Rosetta Stone for understanding the early universe. With the advent of the James Webb Space Telescope (JWST, Gardner et al. 2023), the observational frontier has been pushed to redshifts of $z \approx 10$ and beyond. While JWST is an infrared telescope, the physics it observes is rooted in UV. Due to cosmological redshift, the rest-frame UV light emitted by the early generation of stars and galaxies is stretched by a factor of $(1 + z)$, arriving at the detectors as near- and mid-infrared radiation.

As demonstrated with the early B-type star λ Lep's spectrum[2] in Fig. 2, while the B0.5V type star showing an intrinsic Spectral Energy Distribution (SED) peaks in UV (the black spectrum at $z = 0$), its spectrum is shifted into the infrared bands as the redshift increases. Consequently, for many commonly used filters at $z \gtrsim$1-2 in the optical and near infrared, these observations essentially probe rest-frame UV wavelengths. In this regime, the standard diagnostics of "local" UV stellar physics represent the primary tools for exploring the Epoch of Reionization (EoR). The Lyman-break technique is employed to select candidate galaxies by identifying the abrupt spectral cutoff caused by neutral hydrogen absorption in the intergalactic medium (IGM). Similarly, the UV continuum slope serves as a critical proxy for estimating dust extinction, metallicity, and the age of stellar populations in these high-redshift systems.

However, interpreting these high-redshift data demands accurate rest-frame UV stellar spectra and population models: the stellar IMF, rotation, binarity, metallicity, and nebular reprocessing all imprint themselves on the UV continuum and line spectrum. Uncertainties in UV stellar physics propagate directly into uncertainties in inferred star formation rates (SFRs), stellar masses, ionizing-photon production efficiencies, and even the timing and

curve spectrum is based on the Cerro Paranal Advanced Sky Model (Noll et al. 2012; Jones et al. 2013), with PWV = 2.5 mm and a resolution of $\lambda/\Delta\lambda = 2000$.

[2] λ Lep spectrum from the CALSPEC database: lamlep_stis_008.fits.

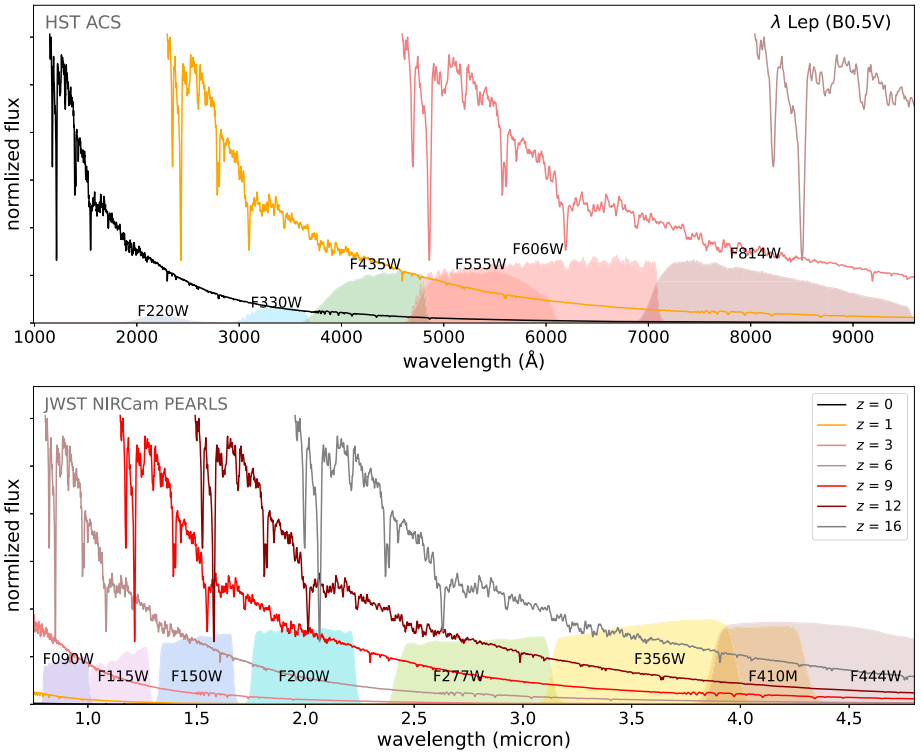

Fig. 2 The spectrum of a B-type star λ Lep (B0.5V) at different redshifts. The photometry bands of selected HST ACS (Ford et al. 2003) and JWST NIRCam bands from the JWST PEARLS program (Windhorst et al. 2023) are also plotted

topology of reionization. In this sense, the "infrared revolution" launched by JWST is deeply rooted in UV astrophysics.

Given this unique role of ultraviolet radiation in shaping our understanding of the universe from the immediate solar neighborhood to the epoch of reionization, we here present a comprehensive review of the UV in stellar physics.

In the following sections, we structure our discussion around the following fundamental scientific questions:

- What physical mechanisms (acoustic waves, magnetic reconnection, Alfvén waves) drive chromospheric, transition-region (TR) and coronal heating?
- How does magnetic activity (flares, spots, chromospheric emission) evolve with stellar age and rotation?
- What is the chemical composition of stellar chromospheres, transition regions and coronae, how it varies with spectral type and is it related to the heating?
- Why is NLTE required in UV stellar-atmosphere studies?
- How can we use UV line diagnostics of NLTE processes to infer how the atmospheric parameters (e.g. temperatures, densities, and ionization conditions) vary with depth and spectral type?
- How does stellar UV/EUV radiation field varies and how it influences exoplanet atmospheric chemistry?

- How can we find and characterise the diverse populations of hot subluminous stars?
- How can we decipher their formation and evolution as well as the processes in their atmospheres from the spectra?
- How and when did this mass-loss arise?
- How was the lost material redistributed in the ISM?
- How was the density perturbation in the ISM created and maintained?

2 The Basics of UV/EUV Stellar Physics

UV spectroscopy provides a uniquely powerful window into the physical conditions of stellar lower atmospheres. Many of the strongest lines of key ions (e.g., C II–IV, Si II–IV, Mg II, Fe II, N V, O VI) lie in the UV, allowing direct probing of temperature, density, and velocity structures in regions inaccessible at other wavelengths for any distant star — from the upper photosphere through the chromosphere and transition region to the stellar wind. UV spectroscopy is therefore an essential tool for models of stellar activity, chromospheric heating, and star–planet interactions via radiation fields and winds. EUV spectroscopy mostly probes the outer layers of stellar atmospheres and has a significant effect on planet atmospheres.

Much of what we know about stellar atmospheres of several classes is based on the little we know about our own star, the Sun. The Solar chromosphere extends from the temperature minimum to the hydrogen ionization limit (∼20,000 K), with UV emission dominated by the highly variable supergranular network. This network structure persists into the thin transition region (TR), a mysterious interface exhibiting systematic redshifts and large non-thermal widths likely caused by radiative cooling flows and line-of-sight effects. However, the TR's extremely low filling factors suggest that much of its emission is physically unrelated to the overlying corona, challenging standard connectivity models. While the solar corona provides abundant forbidden line diagnostics, stellar observations are restricted to the brightest high-temperature transitions (e.g., Fe XVIII, Fe XXI) visible against the disk background.

The Solar and stellar UV has been observed at very high spectral resolution with many instruments. There is ample literature showing that many stars have nearly the same UV spectra and features as the solar ones. For a short review of the solar UV spectral observations see the first section in Del Zanna and Mason (2018).

The UV spectrum is dominated by several continua, mostly from carbon and silicon, and a large number of lines from ions formed in the chromosphere and the transition region, as well as from molecules. They are very difficult to model as outlined below.

Within the HR diagram, it turns out that all stars with convective envelopes produce UV spectra indicating the presence of chromospheres. For example, F-type and cooler main-sequence stars, and at least some late-A stars, show UV evidence for chromospheres. It was once thought that as in the Sun the energy to heat the chromospheres is related to the presence of an inner radiation region, a convective envelope and rotation. However, even fully convective late-M dwarfs and some brown dwarfs show chromospheric signatures. As in the solar case, many stars have cycles of activity. For a review on observational aspects of stellar chromosphere see e.g. Hall (2008).

As the Del Zanna and Mason (2018) review is mostly focused on the EUV we refer the reader to it, and here just point out that the majority of the EUV lines are formed in the TR and corona, i.e. at any temperatures between ∼0.5 and a few MK. There are ample diagnostics to measure the plasma state that are unavailable in the UV. Unfortunately, the only sky survey in the EUV was carried out in the early 1990s with low sensitivity and low

spectral resolution by the EUVE SMEX, hence we know very little in the EUV band about the quiescent coronae of stars (very active flare stars also emit strongly in the X-rays and we have plenty of observations from Chandra and XMM-Newton). There is a misconception that only nearby stars can be observed in the EUV. However, EUVE discovered over 500 sources and we now know that there are far more stars of all spectral type and age that are within a few hundred pc in different directions within the local cavity that are easily observable at the shorter EUV wavelengths.

SIRIUS, proposed to ESA, is a high-spectral resolution mission to fill this knowledge gap by observing wavelengths below 260 Å (see more details about the SIRIUS mission in Barstow et al. 2026, this collection). High-resolution observations of Doppler shifts, densities and especially profiles of coronal lines measured by SIRIUS would provide key information on coronal heating and the role of the dissipation of magnetohydrodynamic (MHD) waves. With Doppler measurements and dimmings SIRIUS will be able to observe coronal mass ejections in stars for the first time.

The First Ionisation Potential (FIP) effect was first noticed in the active solar corona by Pottasch (1963) when analysing Sun-as-as-star EUV fluxes. It is characterised by a relative overabundance of low-FIP elements ($<$10 eV), such as Fe, Mg and Si compared to high-FIP elements ($>$ 10 eV), such as C, N, O, relative to their photospheric values. Whether it is the low-FIP elements that are enhanced or the high-FIP ones that are depleted is still not clear (see the review by Del Zanna and Mason 2018).

EUV and X-ray observations of the hot plasma in stellar coronae have shown a large variety of results, with both FIP and the opposite, Inverse FIP (IFIP) effects present. Various studies (cf. Wood and Linsky 2010; Seli et al. 2022) have indicated a clear correlation of such variations with stellar class, although several results as they have been presented are misleading. First, the Sun shows a bimodal coronal abundance pattern: Plasma at temperatures up to about 1 million K has abundances close to photospheric values, whereas hotter plasma around 3 million K shows a stable FIP bias of about 3, meaning that low-FIP elements are enhanced by roughly a factor of three relative to the photosphere. Secondly, most of the measurements have been taken from high-temperature lines observed in the X-rays, and are not directly comparable to EUV measurements. As chemical variations in the solar lower corona are clearly related to magnetic activity (cf. Laming 2015), EUV SIRIUS observations could provide a significant diagnostic tool of stellar magnetic activity and atmospheric dynamics.

2.1 Atmosphere Modelling

The ultraviolet (UV) spectral window represents the maximum opacity for most hot and intermediate-temperature stars across the Hertzsprung-Russell (HR) diagram. Unlike the optical, which often probes the deep photosphere where conditions may approximate thermodynamic equilibrium, the UV spectrum is formed in the upper atmospheric layers where density drops precipitously. The UV is not only a wavelength range shorter than the optical, it is a regime where LTE often fails badly; for hot luminous stars with strong winds, even hydrostatic and plane-parallel assumptions break down. In this sub-section, we review the modern theoretical framework for stellar atmospheres as constrained by UV observations. We will address the following key questions:

1. Why is NLTE required in UV stellar-atmosphere studies?
2. What physical mechanisms drive chromospheric, transition-region and coronal heating?
3. What is the chemical composition of stellar chromospheres, transition regions and coronae, how it varies with spectral type and is it related to the heating?

4. How can we use UV line diagnostics of NLTE processes to infer how the atmospheric parameters vary with depth and spectral type?

2.1.1 Why NLTE in UV

The foundational assumption for classical stellar atmosphere modeling is that of LTE. This assumption posits that the properties of the stellar plasma at any given point are in equilibrium and can be described by a single, local temperature (T). This includes the particle velocity distributions, atomic excitation, and ionization states. In the LTE regime, the population of atomic levels is governed by the relatively simple Saha-Boltzmann equations. The radiation source function (S_ν) is equivalent to the Planck function ($B_\nu(T)$).

For the most basic case of a two-level atom with complete redistribution, the source function is:

$$S_\nu = (1 - \epsilon_\nu)\, J_\nu + \epsilon_\nu\, B_\nu(T), \tag{1}$$

Here, the J_ν term represents the "scattering" part of the source function, where the radiation field itself dictates the emission, while the $B_\nu(T)$ component is the "thermal" part, where particle collisions (thus the local temperature T) create and destroy photons. The parameter ϵ_ν is the thermalization parameter. Its definition $\epsilon_\nu \equiv \frac{C_{ul}}{A_{ul}+C_{ul}}$ measures the probability that an atom in the upper level (u) will be de-excited by a collision (C_{ul}, the collisional de-excitation rate) rather than by spontaneously emitting a photon (A_{ul}, the Einstein-A coefficient).

The situation of LTE in equation (1) is the case where collisions completely dominate. In a dense environment, such as deep in the stellar photosphere, the mean free path of a photon is short and the radiation field is fully thermalized, so collisions are very frequent. This means the collisional de-excitation rate becomes large, far outweighing the spontaneous emission rate: $C_{ul} \gg A_{ul}$, thus $\epsilon_\nu \approx 1$. The source function S_ν in LTE becomes equal to the Planck function $B_\nu(T)$.

However, the UV spectrum forms in the low-density environment of the outer layers of stellar atmosphere, where the particle density (n_e) drops. Since collisional rates are a function of density, the frequency of these thermalizing collisions plummets. However, the rates of radiative processes (like spontaneous emission, A_{ul}, or photo-excitation, which depends on J_ν) do not depend on the local gas density. Thus $C_{ul} \ll A_{ul}$ and the photon-destruction probability parameter $\epsilon_\nu \ll 1$, leading the source function is scattering-dominated with $S_\nu \simeq J_\nu$. In this case, the source function S_ν is no longer "coupled" to the local gas temperature T (via $B_\nu(T)$). Instead, it is now "coupled" directly to the mean radiation field J_ν. The gas scatters photons instead of creating them thermally (Hubeny 1997; Hubeny and Mihalas 2015; Amarsi et al. 2016).

This decoupling has profound, systematic consequences for UV stellar physics. The high-energy UV radiation field drives ionization and excitation rates that the local thermal pool cannot sustain, necessitating a NLTE treatment:

- Spectral Diagnostics and Abundances: The UV radiation field frequently causes over-ionization (stripping more electrons than Saha-Boltzmann predicts) or optical pumping (populating excited levels via non-local photons). For instance, classical LTE analysis of B type stars yielded contradictory abundances from different ionization stages of Silicon (the "Si discrepancy"; Nieva and Przybilla 2012). NLTE modeling resolved this by correctly predicting the depopulation of Si III and enhancement of Si IV due to the UV field. Similarly, the modern downward revision of solar abundances relies on NLTE corrections to account for UV photo-ionization affecting neutral species (Asplund et al. 2021).

- Atmospheric Structure (NLTE Line Blanketing): The UV opacity is dominated by the "Iron Curtain" of millions of overlapping metal lines. NLTE models account for the over-ionization of species like Fe, which changes the opacity and thus the radiative heating/cooling rates. This leads to the phenomenon of surface cooling and back-warming, altering the temperature stratification $T(\tau)$ of the star. This structural change shifts the entire Spectral Energy Distribution (SED), modifying the ionizing flux budget (Lanz and Hubeny 2007; Martins et al. 2005).
- The Photosphere–Wind Connection: Radiative driving of stellar winds relies on momentum transfer (Castor et al. 1975) through UV resonance lines (e.g., C IV, N V). The strength of this driving force depends critically on the ionization fraction of these species at the base of the wind (Vink et al. 2001). NLTE models can self-consistently solve for the ionization strata that launch and sustain the wind (Kudritzki and Puls 2000), making NLTE a prerequisite for any hydrodynamic study of mass loss.

2.1.2 Modelling the Chromosphere

The solar chromosphere is a complex, non-linearly coupled system extending from the virtually neutral photosphere dominated by hydrodynamics to a fully ionised and magnetically dominated corona. The chromosphere is troublesome as it is dynamic, highly-structured and needs to be described by non-local 3D radiative transfer and NLTE atomic physics. Its dynamics define the structure of the overlying magnetic field. The chromospheric heating feeds the mass-energy cycle of the corona and is dominated by small-scale events with shocks and time-dependent effects being omnipresent. We are very far from being able to model all these eff/ects and understand observations.

The state-of-the-art in current chromospheric modelling of the quiet Sun is provided by BiFROST (Gudiksen et al. 2011), a code that solves the MHD equations with 3D radiative transfer (RT) assuming a static atmosphere, LTE, and a small number of mean opacities. The radiation losses in the chromosphere are calculated with a 1D RT hydro code (RADYN) for the quiet Sun, while the optically thin losses are obtained from the CHIANTI database. Time-dependent ionization for some key elements (H, He) are included. See Leenaarts (2020) for a review. All these codes have generally consistently failed to reproduce the main features of lines and continua in solar regions, see e.g. Kalkofen (2012). The Solar Atmospheric modelling Suite, (SAMS[3]) is a 5-year challenging project funded by STFC (UK) to create advanced models to include all the above effects.

As we do not know the processes forming stellar atmospheres, in order to understand stellar UV spectra we have to start with semi-empirical modeling of the Sun as a star. The common approach has been to create a spectral model for each typical region of the Sun (e.g. cell centres, supergranular network, faculae, sunspots), then create segmentation maps of the solar surface based on images, to estimate the percentage contribution of each region and then combine all to produce an irradiance spectrum of the Sun as a star. The spectral models have been typically created with NLTE RT calculations. Perhaps the best attempt was obtained by Fontenla et al. (2014) after a long series of improvements over decades. Still, agreement in lines and continua was poor. A major problem has always been the UV continua, with order of magnitude discrepancies, requiring the introduction of ad-hoc fudge factors such as extra opacities. An improvement was presented by Haberreiter et al. (2014). A more accurate semi-empirical approach is to estimate irradiances from proxies of solar activity, see e.g. Deliporanidou et al. (2025).

[3] https://sams-project-uk.github.io/.

The UV continuum and lines from neutrals/singly ionised atoms are emitted by the photosphere and chromosphere, although their formation is strongly affected by photo-ionization originating from all layers of the atmosphere, and by recombination from ions present in the transition region. The hydrogen and helium lines are most affected and have been the most difficult to model. The lower lines of the hydrogen Lyman series up to ϵ are optically thick and self-reversed. Proper modeling of neutrals and singly-ionised atoms would require large collisional-radiative models (CRM) where at least 2-3 charge states are included. Such models have never been developed nor coupled with RT and MHD. CRM for hydrogen and helium with some opacity effects have only been developed to study astrophysical nebulae. The first CRM model for the solar outer atmosphere was developed by Del Zanna et al. (2020) for helium.

2.1.3 Modeling Transition-Region Lines

Plasma diagnostics based on UV TR lines are very limited, as discussed in (Del Zanna and Mason 2018). On the other hand, the strongest TR lines are in the UV. It has long been known that the modeling of the lines from the 'anomalous' ions, belonging to the Li- and Na-like sequences (such as Si IV, C IV) under-predicts their radiance by large factors (2–6) compared to those from other ions forming at similar temperatures. This problem was present even in the analysis of the earliest irradiance observations by Pottasch (1963), although noticed a decade later (see the review in Del Zanna and Mason 2018).This problem was not noticed for a long time when analysing UV stellar spectra. It was only by combining observations of AU Mic by several instruments with lines from many sequences that it was shown for the first time that the problem was clearly present in stellar UV spectra (Del Zanna et al. 2002).

The collisional and radiative rates for the strong lines were known relatively well even in the 1970's. The problem with their modeling lies primarily with the ion balance: at TR densities, density-dependent effects (suppression of dielectronic recombination and ionization from metastable states) and charge transfer shift the formation temperature and increase the line radiances by large factors. The physics has been known for a long time and a few of these effects were included in some solar studies with various approximations (see the review by Del Zanna and Mason 2018). Within stellar physics, Sim and Jordan (2005) developed a very approximate ionisation equilibrium by including density and charge transfer effects for some carbon and silicon ions and showed improvement in 1D emission measure analyses of UV observations of the K2 V dwarf star ϵ Eri.

Improved modelling was developed by G. Del Zanna, with contributions from his PhD student R. Dufresne. Given the limitations in the available atomic data, various approximations needed to be implemented; details and references can be found in the CHIANTI version 11 paper (Dufresne et al. 2024), where such advanced ionization equilibrium models for several elements have been made available to the community. The analysis of a solar plage UV spectrum showed significant increases, nearly resolving all inconsistencies. For example, the radiances of the Si IV lines were increasd by a factor of 6.

Clearly, considering its dynamical and spatial structure, modelling the TR would require the inclusion of time-dependent effects, but even the current models still need improvements.

The CHIANTI version 11 advanced models were applied by Deliporanidou and Del Zanna (2024) to analyse HST/STIS observations of a range of stars spanning the HR diagram: ϵ Eridani (K2 V), α Centauri A (G2 V), Procyon (F5 V) and Proxima Centauri (M5.5 Ve). This allowed the first measurement of the FIP effect in stellar TR. The resulted relative elemental abundances were compared with up-to-date photospheric abundances, showing no evidence for the FIP effect in the TR of this stellar sample, as expected on the basis of

the solar results (Del Zanna and Mason 2018) but in contradiction to the claim that stellar atmospheres have an FIP effect that varies with spectral type. It is now known that the TR of the Sun and stars have little variability with the activity cycles (see, e.g. Del Zanna and Andretta 2015; Ayres 2015), which may be one reason why the FIP effect is not present.

2.1.4 Modelling Coronal Lines

Modelling coronal lines is relatively straightforward, as they generally have little opacity effects, hence can be calculated in the optically thin regime. As in the case of the Sun, modelling stellar EUV fluxes of coronal lines can be achieved with some form of emission measure modelling, if enough information is available, or with activity proxies (see, e.g. Namekata et al. 2023; Deliporanidou and Del Zanna 2024). As EUV fluxes have a fundamental effect on exoplanet atmospheres (cf. Linsky 2019), accurate modelling is important.

2.1.5 Shortcomings in Atomic Data and Radiative Transfer Modelling

The main processes requiring atomic data needed to build collisional-radiative models are:

1. Collisional excitation (CE) by electrons and protons;
2. Radiative rates for spontaneuous emission;
3. Collisional ionisation (CI) and photo-ionisation (PI) from populated states;
4. Charge transfer (CT) interaction with neutrals (mainly H,He);
5. Radiative recombination (RR) from populated states to all states;
6. Dielectronic recombination (DR) from populated states to all states, corrected with its suppression due to density effects;
7. Photo-excitation (PE).
8. Other parameters are needed such as line broadening.

Since the 1960s semi-empirical 1D static atmospheric models have been developed with simple RT codes and approximate small atomic models. PANDORA, written by Loeser under the guidance of Avrett at CfA, formed the basis of many following codes, which provided standard atmospheric models still widely used such as the VAL (Vernazza, Avrett, Loeser), see e.g. Vernazza et al. (1973) and FAL (Fontenla, Avrett, Loeser), see e.g. Fontenla et al. (1990). Significant improvements such as the multilevel accelerated lambda iteration (MALI) method were developed by Rybicki and Hummer with a series of papers, one being Rybicki and Hummer (1992). MULTI is another widely-used code (Carlsson 1986), recently extended to 3D, but within solar physics the most widely used code is the RH (named after Rybicki and Hummer) code (Uitenbroek 2001). Within astrophysics, many RT codes have been written such as TLUSTY (see Hubeny and Lanz 1995, and following papers), whilst a recent one is MCFOST (Tessore et al. 2021). For a review of some of the RT methods see e.g. Hubeny and Mihalas (2015), Rutten (2021) and references therein.

Something all the RT codes have in common is the lack of updated atomic rates and atomic modelling, as recently pointed out in Dufresne et al. (2025). The CE rates commonly used are often semi-empirical impact-parameter or g-bar approximations used in the 1960s and early 1970s. Even in the few cases when better atomic data were used, the fundamental limitation is that it is very difficult to accurately calculate collision (and radiative rates) for neutrals (and singly ionised atoms) even with the most sophisticated codes. Hydrogen CE rates are emblematic: all the RT codes still use incorrect rates, and all the published calculations have their own limitations, as discussed by Del Zanna et al. (2025a). Several groups used to provide accurate CE rates with R-matrix scattering codes. The UK Atomic

Processes for Astrophysical Processes (APAP) Network[4] produced rates for all ions from the H- to Mg-like isoelectronic sequences, recently revised by Del Zanna et al. (2025a). In addition, complex heavy ions require large scale scattering calculations such as those carried out to provide data in the 50–170 Å region (see references in Del Zanna 2012). The CE rates produced by the UK APAP network cover about 90% of all the published rates for astrophysical ions included in atomic databases, see e.g. CHIANTI v.10 (Del Zanna et al. 2021). However, most experts passed away (cf. Del Zanna et al. 2025b) or retired.

Accurate radiative rates for low-lying bound states are now available for most atoms/ions, calculated with the Multi-Configurational Hartree–Fock (MCHF) approach, pioneered by the late Charlotte Froese Fischer (cf. the ATSP program Froese Fischer et al. 2007), or with the multi-configuration relativistic Dirac-Fock (MCDHF) method, pioneered by the late Ian P. Grant (cf. the GRASP program; Grant et al. 1980), but rates for high-lying states are mostly missing.

CI rates from ground states are relatively well-known as they have also been measured experimentally, but those from excited states are not. Moreover, most RT codes still include electron impact ionisation rates calculated with approximate formulae.

CT rates generally adopted in RT codes were calculated with very approximate methods unsuitable for chromospheric temperatures. Updated rates have been collected from the literature and made available via the CHIANTI database v.11 (Dufresne et al. 2024).

The main improvement in RT codes was the inclusion in the 1980s and 1990s of accurate photo-ionisation (PI) cross sections produced by the Opacity Project (OP, Seaton 1987). These data are still state-of-the-art R-Matrix calculations in LS coupling, but are summed over the final states. One problem is that these cross sections have been used within the RT codes to calculate the inverse process of radiative recombination (RR), which is incorrect. Badnell (2006) calculated with the distorted wave (DW) approximation (which does not take into account resonances related to auto-ionising levels) initial and final-state resolved RR rates for all ions in the sequences from H-like up to Mg-like for all elements up to Zn. Calculations have been later refined and level resolved PI cross sections calculated from them and made available at the UK APAP website. These PI cross sections should be used within RT codes as carried out in Dufresne et al. (2025). These cross-sections plus additional ones in a format compatible with the CHIANTI data have been made available on ZENODO as described in Dufresne and Del Zanna (2026).

DR rates have usually been neglected in RT calculations or just the Burgess formula Burgess (1964) has been used, which is only valid at coronal temperatures. Level-resolved DR rate coefficients were calculated for all H- to P-like ions as part of the DR Project (Badnell et al. 2003) and are available on the UK APAP website. However, DR rates are strongly damped at high densities. Only approximate estimates of this DR suppression have been used in the literature, all derived from hydrogenic models developed by A. Burgess in the 1960s and the results published in Summers (1974). Such estimates are not reliable at low temperatures. Generally, most DR calculations are anyway inaccurate at chromospheric temperatures, as originally shown in his seminal paper by Storey (1981) and in a few following studies. Calculating low-temperature DR is very difficult. The last project of the UK APAP network was to calculate DR for the very complex iron ions, as iron is fundamentally important in astrophysics. The first paper (Zhang et al. 2025) discussed the higher charge states where one laboratory measurement is available. The second paper presents the calculations of the even more complex lower charge states.

[4] https://www.apap-network.org/.

However, the main limitations of all the atomic models used in RT calculations are the small sizes of the atoms, limited to a few states, neglecting all the recombination and radiative cascades from the states not included. The improvement of the atomic models included by Dufresne et al. (2025) resulted in a factor of 10 decrease in the UV continuum without any fudge factors, resolving a discrepancy that has been present since the 1960s. Clearly, improving atomic models is a necessary step.

Finally, it is important to point out that a large number of EUV/UV lines are still unidentified and almost all of them do not have accurate reference wavelengths.

2.1.6 Lines from Neutrals: New Diagnostics

Diagnostics for the solar upper chromosphere have generally been limited to Mg II h and k, Ca II H and K, and hydrogen Hα. For the lower chromosphere, UV continua and some molecular lines have been used to probe the atmospheric conditions around the temperature minimum region.

The UV spectral range is full of hundreds of emission lines from neutrals, many of which are unidentified (cf. Sandlin et al. 1986) but could potentially be used as diagnostics of the chromosphere. Only a few from the lower states have been studied with NLTE RT calculations, the notable ones being the C I 1355.8 Å line emitted from the $2s^2\,2p\,4f\ ^1D$ state (Lin et al. 2017) and the O I 1355.6 Å intersystem line (Lin and Carlsson 2015). These lines are estimated to be formed in the mid-chromosphere. The modelling carried out by the authors is complex but still the C I line is predicted to have a strong self-reversal, which is not observed.

A large fraction of lines from neutrals in the UV are however emitted by Rydberg states. These lines have not been studied until recently. The hydrogen CRM model developed by P.J. Storey (Hummer and Storey 1987; Storey and Hummer 1995) and the helium one developed by Del Zanna et al. (2020) indicate that levels within neutrals having principal quantum number higher than $n = 10$ are in local thermodynamic equilibrium (LTE) with the ground state of the singly-charged ion in the solar chromosphere. This simplifies enormously the modelling, as the populations of the Rydberg states can be calculated with the Saha-Boltzmann equation; the local emissivities of the Rydberg lines can then be calculated once the A-values are known. As previously mentioned, general atomic structure codes fail to produce such values. One way to calculate accurate A-values for the Rydberg lines in neutrals is to use the R-matrix codes and the frozen core approximation, as carried out by Storey et al. (2023) for neutral carbon, where data for states up to $n = 30$ were calculated. Opacity effects still need to be included, either with escape factors as shown in Storey et al. (2023) or with a full RT calculation as shown in Dufresne et al. (2026). Rydberg lines from carbon are predicted to be formed between the temperature minimum and the mid chromosphere, offering new diagnostics in this poorly study region, for the Sun and other Stars.

We are clearly a long way to even attempt a physical understanding of the solar chromosphere and transition region. There is not much hope to resolve the coronal heating problem without understanding the main physical processes occurring in the chromosphere. The fine structure and the dynamics of these regions clearly indicate that all previous models of plane-parallel static atmospheres are not realistic. The SAMS project will deliver open-source codes with additional physics and the community will be welcomed to contribute.

Until we understand the solar atmosphere there is not much hope to understand stellar atmospheres. However, EUV/UV observations of stars do provide useful information on how magnetic activity evolves with stellar age and rotation, and given the strong influence of the UV/EUV radiation field on exoplanet atmospheric chemistry, modelling stellar fluxes is important.

Scientific advances will be achieved by combining high-spectral resolution observations with advanced modelling. We have given a few examples of how relatively simple atomic modelling can provide significant improvements, opening the potential for many unexplored spectral diagnostics in the UV. New missions need a supporting infrastructure, e.g. laboratory astrophysics, atomic and molecular physics – measurements and theory, and improved physics modelling, but most importantly a critical mass of well-trained researchers, without which the science outcomes cannot be achieved.

Laboratory astrophysics support was strong in the 1970s and 1980s but has almost completely disappeared. Knowledge in atomic physics has disappeared in most countries. For example, the CHIANTI database has become the international reference for atomic data but was developed by a few with almost no financial and no community contributions. Similarly, all other atomic databases for astrophysics have relied on efforts by singles for improvements. There is a lack of international coordination. Very little atomic rates are calculated nowadays, also because the work of the producers is never acknolwedged, whenever data are ingested in atomic databases. In essence a situation not sustainable for the future.

3 The Afterlife of Stars with UV

3.1 Studying Hot Subluminous Stars in the Ultraviolet

The evolution of stars is still not completely understood. In particular, the region of the hot subluminous stars (sdO/B/A) located in luminosity between the main sequence and the white dwarfs remains as one of the last uncharted territories despite the fact that no less than 97% of all stars are evolving through this region at some point during their lives. The main reasons are short evolutionary timescales or peculiar evolutionary channels. Entirely new types of stars have been and are still being discovered, whose formation and evolution are often unclear. About 20 new types of objects were found within the last twenty years only.

The zoo of hot subluminous stars is quite diverse. Most stars are entering the hot subluminous regions after they have passed the asymptotic giant branch (AGB). However, the evolution becomes so fast that only relatively few objects are observable on this post-AGB speedway. Close binary interactions are invoked to explain the formation of other types of hot subluminous stars (Heber 2016). Because their envelopes are stripped by mass-transfer to a binary companion during or even before the first giant phase, those stars are either in the relatively stable helium-burning phase (extreme horizontal branch, EHB) or they are slowly cooling down to become helium WDs. Since the existence of single and helium-rich types of sdO/Bs seems to be inconsistent with them being stripped by companions, diverse merger scenarios involving He-WDs in tight binaries have been invoked to explain their formation.

Hot subluminous stars also play an important role in a broader context. Likely formed by different types of stellar interactions, they are suited to explore those interactions. Their atmospheres are chemically peculiar and serve as laboratories to study mixing, mass loss, and diffusion processes. They are regarded as important contributors to the UV-excess seen in early-type galaxies and are crucial to understand the HB morphology and evolution of globular clusters. Stripped stars of intermediate mass are regarded as important to explain the reionization of the Universe. Some of the diverse types of pulsators among the sdO/Bs are well suited for asteroseismic modelling. And close binary sdO/Bs are among the best candidates for the progenitors of type Ia supernovae and sources for gravitational wave radiation detectable with space-based instruments.

3.1.1 The Role of UV Surveys to Detect sdO/Bs

Hot subluminous stars are bright in the ultraviolet (UV). Already, the first dedicated surveys to search for those "faint blue stars" used near-ultraviolet bands observable from the ground to identify them (Humason and Zwicky 1947). UV surveys from space lead to the discovery of new sdO/Bs. The first all-sky UV survey was conducted with the S2/68 telescope on the ESRO satellite TD1, which provided low-resolution spectrophotometry down to visual magnitudes of ~ 10 mag and found ~ 1500 candidate sdO/Bs (Carnochan and Wilson 1983). The first published scientific analyses of sdO/Bs were based on pointed observations with a spectrophotometer on board the Netherlands Astronomical Satellite (ANS) (van Duinen et al. 1975; Wesselius et al. 1976).

The Very Wide Field survey of UV-excess objects conducted with a camera onboard Spacelab-1 covered about half of the celestial sphere down to 9.3 mag and also led to the discovery of some sdO/Bs (Viton et al. 1988). An objective prism telescope surveyed $\sim$ 9% of the sky operated from Skylab during the manned missions, and among the observed sdO/Bs was the first composite hot subdwarf with MS component showing a UV-excess (Laget et al. 1978). The FAUST far-ultraviolet imager observed 4% of the sky during the NASA ATLAS-1 mission and detected several sdO/Bs (Brosch et al. 1995).

The catalogue of the all-sky GALEX mission was used and is still in use to select sdO/Bs (Vennes et al. 2011; Geier et al. 2019). Although state-of-the-art catalogues of hot subluminous stars are now compiled based on Gaia data, a combination with UV photometry is still advantageous, especially when searching for UV-excesses in composite systems (Dawson et al. 2024). The UVIT telescope on board of the ASTROSAT observatory (Subramaniam et al. 2016) and the UVOT telescope onboard Swift observatory (Gehrels et al. 2004; Rao et al. 2022) are used to detect such excesses caused by sdO/Bs in pointed observations of clusters. Finally, HST photometry allowed us to observe much fainter objects and revealed the complex populations of EHB stars in globular clusters (Piotto et al. 2015) as well as a hidden population of intermediate-mass sdOs in the Magellanic Clouds (Drout et al. 2023).

Significant progress has been made in tackling the main science questions by detecting hot subluminous stars in different populations, where new types are still discovered.

3.1.2 UV Spectroscopy as Key for Detailed Characterisation

The first UV spectra of hot subluminous stars taken with the S2/68 instrument have been shown by Carnochan et al. (1975). However, the era of UV spectroscopy of sdO/Bs started with IUE, which allowed for the first time pointed high- and low-resolution spectra to be obtained for a substantial number of objects. SdO/Bs were already included as commissioning targets (Heap et al. 1978) and the first quantitative spectral analyses in the UV were performed using IUE data (Heber et al. 1984) and led to several key discoveries.

The first metal abundance patterns measured in the UV (Baschek et al. 1980; Lamontagne et al. 1985) confirmed sdO/Bs to be chemically peculiar, and diffusion processes were invoked to explain those patterns. Mass loss by stellar winds in luminous sdOs was first detected in the UV (Hamann et al. 1981) as well as the first stripped sdO next to a Be type star (Thaller et al. 1995). The crucial role of UV spectra to improve model atmospheres and address issues such as the uncertain temperatures of the hottest sdO/Bs or the Balmer line problem became apparent (Werner 1996).

FUSE spectroscopy (see Fig. 3) extended the available wavelength range downwards and allowed to measure the abundances of more and heavier elements (Ohl et al. 2000). A few sdO/Bs have also been observed by the ultraviolet spectrometers on board of the

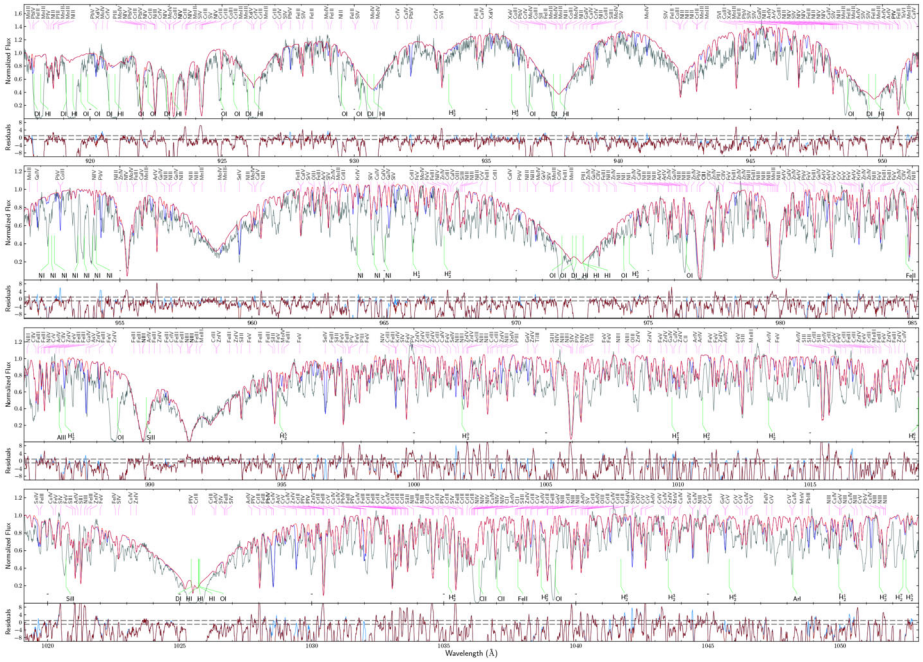

Fig. 3 FUSE spectrum of the intermediate He-sdOB HZ 44 (gray) with the best model (red, with heavy metals: blue) from Dorsch et al. (2019)

Voyager spacecrafts (Wesemael et al. 1985) and the TUES echelle spectrograph attached to the ORFEUS telescope deployed by the space shuttle (Rauch and Strauß 2025).

The improved sensitivity of HST allowed for more detailed studies, also for fainter stars, already starting with the GHRS spectrograph (Lanz et al. 1997; Gies et al. 1998). STIS spectra were used to show that the surface abundances of iron-group elements do not influence the pulsation properties of sdBs (O'Toole and Heber 2006) and to provide the full abundance patterns of super-metal-rich He-sdOBs (Dorsch et al. 2021). COS spectra were used to perform the first detailed studies of sdO/Bs in globular clusters (Chayer and Dixon 2014; Latour et al. 2017). UV spectra of sdO/Bs have also been used to improve atomic data for iron-group elements (Landstorfer et al. 2024).

3.1.3 Scientific Objectives

All of those results illustrate the progress made in characterizing UV-spectra of sdO/Bs both on the observational and on the modelling side. UV photometry and spectroscopy play a crucial role in solving the open questions related to the formation and evolution of hot subluminous stars, and with that, the role of interactions for the evolution of stars in general.

- Detecting all of the hot subluminous stars, including the ones which only reveal themselves through weak UV-excesses next to much brighter companions, in different Galactic and extragalactic populations, is necessary to put constraints on the frequency of diverse types of interactions. It is predicted by theory and has been shown by observations that the binary properties of sdO/Bs differ between those populations (Geier et al. 2024). Studying those differences will allow us to understand the underlying interactions better. Clusters

are of special importance because they allow us to put stricter constraints on the progenitor properties. To probe the Galactic halo, the bulge, open and globular clusters, as well as satellite galaxies, we need deeper photometric UV surveys with higher spatial resolution to mitigate crowding.

- The UV is the only wavelength range where abundances of heavy and even trans-iron elements are detectable in hot subluminous stars, and the best to determine their metal abundances in general. Those abundance patterns give important clues for potential formation channels, where episodes of stripping or mixing are involved. Very recently, it has been shown that the abundance patterns of some peculiar He-sdOBs are consistent with predictions from i-process nucleosynthesis models (Battich et al. 2025). If confirmed, this will not only help to constrain the evolutionary history of those stars but might have much wider implications for the origin of the heavy elements in the Universe.
- The atmospheres of sdO/Bs show many peculiarities, which make them ideal laboratories to study hot, radiative atmospheres in general. Their compositions can be so extreme that the structure of the atmosphere is changed significantly, radiative levitation and gravitational settling play a role, vertical stratification and Zeeman splittings have been observed, some sdOs show weak and potentially metallic winds, and many of the spectral features in the UV still remain unidentified due to the lack of atomic data. Hot subluminous stars are therefore ideal testbeds to improve models for hot stellar atmospheres and have been used to that end ever since.

3.1.4 Future Prospects and Needs

Access to UV spectrographs with resolutions sufficiently high to resolve the spectral features is needed to make further progress along those lines. It has to be pointed out that archival UV spectra of sdO/Bs have a particularly high legacy value. The archival collections of IUE, FUSE, and STIS are still in use to test improved models. It is therefore crucial to keep those collections publicly available. The growing diversity of hot subluminous stars, where new discoveries are still made, calls for a significant extension of this collection, ideally covering the full diversity of those objects. The recently completed STIS/COS treasury program 17697 observed 37 sdO/Bs of diverse types and marks an important step in this direction.

It has to be pointed out that it is mostly the lack of atomic data for many species that limits the diagnostic value of the spectroscopic data we have at hand. Theoretical and experimental research in this direction needs to be maintained and extended to make further progress.

3.2 Planetary Nebula

Planetary Nebulae (PNe) are critical laboratories of late stage stellar evolution of low-to-intermediate mass stars (1–8 Msun) as they transition to white dwarfs. Though they are short lived (5000–20,000 yrs) phase, e.g. Badenes et al. (2015), they provide a key, co-eval snapshot of stellar death. Their progenitor stars dominate all stars above one solar mass, so PNe, via their ejecta, are responsible for a large fraction of the chemical enrichment of the interstellar medium (ISM), strongly shaping galactic chemical evolution given their numerical dominance, e.g. Maciel et al. (2015), Stanghellini and Haywood (2018). The numbers currently known in our Galaxy remain modest, $\sim$ 4000 and as recorded in the MASH and then HASH database, e.g. Parker et al. (2006), Miszalski et al. (2008), Parker et al. (2016). Their shells are effectively ionised plasma and so PNe exhibit a rich, strong emission-line spectra across a wide range of the electromagnetic spectrum including in the UV. This enables them to be detected out to large distances in our own Galaxy and in the closer external galaxies,

e.g. Reid and Parker (2006, 2013) for the Magellanic Clouds and Bhattacharya et al. (2019) for more remote examples. Indeed, PNe are a key observational tracer of distant low-mass stars. PNe emission lines also allow determination and analysis via high S/N spectroscopy quality chemical abundances, e.g. Tan et al. (2024). Estimation of shell expansion velocities and ages can also be straightforwardly measured, e.g. Gesicki and Zijlstra (2000), so permitting the probing of the physics and timescales of stellar mass loss. Measured PNe radial velocities can trace their kinematic properties permitting us to determine if they belong to a younger or older stellar population, e.g. Smith et al. (2017). The kinematic properties and visibility also make PNe useful kinematical probes for understanding the structure of galaxies, and to test whether a galaxy contains a substantial amount of dark matter. The PN formation rate also provides the death rate of stars born billions of years ago and so they directly probe Galactic stellar and chemical evolution. They exhibit a wide variety of complex morphologies that also provide clues to their formation, evolution, mass-loss processes, and possible shaping role by magnetic fields (Sabin et al. 2015) and binary central stars (De Marco 2009; Hillwig et al. 2016). As the central star fades to become a white dwarf and the nebula expands, the integrated flux, surface brightness and radius change in ways that can be predicted by current stellar and hydrodynamic theory (Dopita and Meatheringham 1991). However, key physical processes—such as mass-loss mechanisms, ionization dynamics, and the role of binarity in shaping nebulae—remain poorly understood. A dedicated ultraviolet (UV) space based telescope equipped with a UV optimised spectrograph can address these gaps. A key feature is that the central stars of PNe (CSPNe) emit predominantly in the UV, and critical diagnostic lines for gas/dust physics also lie in this regime which is accessible only from Space. For an excellent review of the PN phenomena see Kwitter and Henry (2022) and for how to identify them Frew and Parker (2010) and how to find them Parker (2022), see Fig. 4, including from existing narrow-band surveys (Parker et al. 2005; Drew et al. 2005, 2014).

3.2.1 Selected Scientific Objectives

Below a selection of key scientific objectives that can be tackled in late stage stellar evolution in general and planetary nebulae and their hot, central stars in particular via UV studies are briefly described.

- Ionization and Dynamics: High-resolution UV spectroscopy will resolve velocity structures (e.g., shocks, winds) via lines like C IV (1548–1550 Å) and O VI (1032–1038 Å), probing the interplay between CSPNe winds and nebular expansion.
- Chemical Abundances: UV-sensitive emission lines (e.g., C III], O III], N IV]) enable precise measurements of CNO abundances, crucial for constraining nucleosynthesis and AGB nucleosynthetic models.
- Central Star Properties: UV continuum and absorption features will determine CSPNe temperatures ($\geq$30,000 K), luminosities, and mass-loss rates, critical for evolutionary models.
- Morphological diversity: High spatial resolution UV imaging coupled with spectroscopy can resolve collimated outflows and ionization fronts, testing the binary hypothesis for shaping and interaction with magnetic fields for fundamental shaping of bipolar PNe.
- Dust and Molecular Gas: Far-UV absorption edges (e.g. 2175 Å bump) and electronic transitions (e.g. H_2, PAHs) map dust composition, destruction zones.
- Temporal Evolution: Time-domain UV monitoring will track CSPNe variability (e.g., pulsations, wind fluctuations) and nebular recombination timescales.

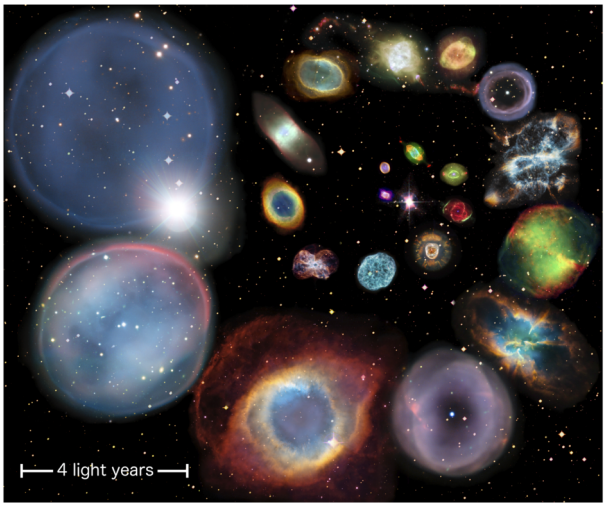

Fig. 4 An iconic montage of 22 well-known PNe, arranged in a spiral pattern by order of approximate physical size. Each nebula's size is calculated from the SB-r statistical distance scale from Frew et al. (2016). It can be applied to PNe exhibiting the entire range of surface brightness, morphology and size. The largest PNe have a surface brightness about a hundred thousand times fainter than the smallest and can reach up to 3 pc across. General image credit: ESA/Hubble and NASA, ESO, NOAO/AURA/NSF. Names of these PNe starting at the top left hand corner and following the spiral are: Abell 33, K 1-22, NGC 7293, IC 5148/50, NGC 2818, NGC 6853, NGC 5189, IC 4406, Shapley 1, IC 289, Fleming 1, NGC 3132, IC 4406, NGC 6720, NGC2440, NGC 1501, NGC 2392, NGC 6543, NGC 6826, NGC 7009, IC 418, NGC 7027, HD 44179). Image reproduced with permission from Parker (2022), copyright by the author

3.2.2 Some Proposed Technical Requirements

Desired spectral Capabilities should ideally cover the Far-UV (900–1700 Å) and near-UV (1700–3000Å) with R $\geq$ 5000 (and ideally much higher) for spectroscopy in order to resolve some key line profiles and weak emission features. Overall system sensitivity should be able to detect faint emission lines, e.g. flux $\leq 10^{-15}$ erg/s/cm^2, especially for distant and extended PNe of low surface brightness. Furthermore it would be advantageous to be able to undertake multi-epoch Observing via a system of flexible scheduling so as to be able to monitor temporal changes on timescales of days to years. This would initially be for a carefully selected high value PNe targets.

3.2.3 Broader Impacts

UV spectroscopy can help revolutionize understanding of stellar feedback, ISM enrichment, and white dwarf formation. Data will also benefit hot star winds, exoplanet host star environments (via white dwarf metal pollution studies), and dust life-cycle models. By addressing questions in late-stage stellar evolution, these data will complement JWST and ALMA observations, providing a complete picture of matter recycling in galaxies. In conclusion a new medium aperture UV optimised Space telescope, such as that proposed by elements of the Chinese astronomical community and as championed by CIOMP(Changchun Institute of Optics, Fine Mechanics and Physics), with a photometric and spectroscopic capability is imperative to unlock the secrets of PNe. Such a facility would offer unprecedented insights into the final acts of stellar lifecycles. The proposed instrument will fill a critical gap in UV astrophysics, ensuring Chinese leadership in stellar evolution research.

3.3 UV Emission in Supernovae Remnants (SNRs) and Their Correlation with X-ray Emission

Supernova remnants (SNRs) play a vital role in galaxy evolution. Besides influencing the dynamics and kinematics of the ISM, the shock wave and ejecta also enrich it by mixing in the nucleosynthetically processed material from the pre-supernova progenitor. Most importantly, SNRs serves as records of historical galactic star formation. Constraints on models of late time shock–ISM interaction aside, their study also provides an insight in to the as-yet poorly understood evolutionary state of the pre-SN progenitor and its CSM. Deep (up to Msec) Chandra X-ray imaging of several SNRs have highlighted several complex phenomena, both resolving and raising questions about (a) progenitor environment and shock interaction, (b) progenitor ZAMS and metallicity and (c) the nature (clumpy, gaseous, or dusty) and the physical properties of the ISM itself. Evolving SNRs ($<$ 10,000 yr) tend to be both optically and X-ray bright, with the X-ray emission attributed to heated gases ($T \sim 10^{6-7}$ K, possibly by a reverse shock) contained within a cooling (10^{4-5} K) shell. Complementing the X-ray and optical observations with UV, allows us to uniquely assign an origin (ISM, CSM or ejecta) to each component of its morphology (knots, filaments, X-ray bright streamers etc.), in turn leading to a complete picture of the supernova event and its evolution.

One of the most pressing questions in stellar physics, galaxy evolution and heavy metal abundance, is the one linking terminal fate of one generation of stars with the birth of the next generation. While it is broadly understood that the matter generated via nuclear burning in stars must be redistributed in to the interstellar medium (hereafter, ISM) via some form of mass-loss (continual, episodic or terminal), and that next generation of stars must arise from this enriched material, via density perturbations induced in the ISM, this picture is far from complete. The ISM serves as an excellent laboratory to study shock dynamics, as well as to carry out stellar archaeology, in order to search for traces of stellar explosions over the last 10^6 yr and more. It consists of matter at temperatures ranging from $10 - 100$ K (cool, molecular clouds comprising primarily of neutral Hydrogen) to 10^4 K (warm, partially ionized gases), to 10^6 K (coronal gases from stars, and other, strongly ionized, media, generated via supernovae and their shocks). The densities range from 10^6 to 10^{-2} cm^{-3}. From the viewpoint of stellar archaeology, the warm, and hot, ionized media, are the most interesting as they comprise primarily of nebular structures, created via mass ejections from a previous generation of stars at various evolutionary stages. Clearly, enrichment of the ISM must occur in the final stages of shock dissipation, but again, the mechanism is poorly understood, and merits a further study.

Among the more important questions that remain unanswered are:

- How and when did this mass-loss arise?
- How was the lost material redistributed in the ISM?
- How was the density perturbation in the ISM created and maintained?

All of these questions are also intricately connected with the terminal, explosive, stages of stellar evolution, which is a process not yet well understood. Moreover, non-terminal mass loss, plays an equally important role via the as-yet poorly understood physical processes which lead to partial ejection of the envelope of massive stars ($> 8M_{\odot}$), several centuries to decades prior to the terminal supernova explosion. With explosion energies of up to 10^{51} erg, supernovae (hereafter, SNe) of all kinds are obviously the most energetic origins of the blast wave, leading to shocks with initial velocities of up to several times 10^4 km s^{-1}, eventually reducing down to a few $\sim$ 100 km s^{-1} as it rams through the low density ISM. Thus, the next question is: How does the shock deposit its energy into the ISM, and what are the most

appropriate conditions under which the maximum transfer of energy takes place? Briefly, the temporal evolution of an SNR covers four stages: (a) the free expansion phase, lasting for $\sim$ several $\times 10^2$ yr (dominated by thermal emission) (Chevalier 1977), (b) the adiabatic (Sedov–Taylor) expansion phase, which is reached when $M_{\rm ISM} \simeq M_{\rm ejecta}$, (X-ray / FUV line emission and thermal bremsstrahlung), with a duration of $\sim 10^4$ yr, (c) The "snow-plow" phase (up to 10^5 yr), dominated by radiative cooling, is reached when $M_{\rm ISM} \gg M_{\rm ejecta}$, and $T \leq 10^5$ K, leading to optical and UV line emission, and finally, (d) the final mixing the ISM and ejecta (De Pasquale et al. (2010) and references therein). The duration for which an SNR remains in each phase, and its multi waveband spectra, is determined by strength of the SN shock, the $M_{\rm ejecta}$ and the density of the CSM. All of these in turn depend on the properties of the unknown progenitor, as well as on the mass and thermodynamic properties of the ISM.

Observationally, SNRs have been seen to brighten in different electromagnetic bands, as they age. Young SNRs are X-ray bright but faint in the UV/optical/IR bands, with X-ray spectrum in 0.3–10 keV bands dominated by thermal emission from a plasma in a state of non-equilibrium (i.e. the thermal profile of e^- is distinct from that of the ions) ionization. Gases at the leading edge of the shock front cool more rapidly, and the interaction of the shocked, cooling, gases with the ISM produces structures resembling flames, filaments, knots, sheets and filaments that we typically associate with SNRs in the UV/optical/IR bands.

Overall, in each emission band, an SNR can be center-filled, or shell-like (or a combination of both), with recent 1-D magneto-hydrodynamical simulations implying that an aging remant can morph from one type to another (RaTPAC simulation, Brose et al. (2021)). This implies that, in addition to a changing peak emission band as SNR evolves from free expansion phase to the Sedov phase, when the swept up ISM at the shock front contributes to its emission, the remnant's structure as seen in each band – radio, IR/optical/UV, X-ray and γ-ray, also changes from one type to another. SNR ages, usually estimated directly from expansion velocities (e.g. the X-ray expansion of Cas-A (Koralesky et al. 1998)), are subject to many uncertainties. The primary assumption therein is that the ejecta is expanding in to a near-uniform ISM. However, as a recent study of previously unidentified nebular structures located in regions of low galactic extinction (Fesen et al. 2021), shows, it is possible for a relatively young SNR to have slow-moving shock fronts with v $\sim$ 70 to 100 km/s, implying an anomalously large extent. Such a situation is possible only if the SN-ejecta expands in to a relatively low density environment, e.g., a low density bubble created by slow (compared to SN shock velocities) moving winds from the progenitor. Shock dissipation via cycles of ionization and recombination peak within the walls of this cavity, as forward and reverse shocks are refracted by the inhomogeneous layers of material located there. Such a scenario has now been proposed for the near completed shell like Cygnus loop, which is proposed to be the remnant of a core-collapse supernova in a late-O / early B-type stars (see Fesen et al. 2018 and references therein). The structural asphericity is attributed to a sharp drop in density in southern walls of the cavity. However, this model does not explain the limb-brightened X-ray emission seen from north-south interface region seen in my own observations of the Cygnus nebula. Note that while the progenitor mass implies a core-collapse explosion, no central compact object (CCO) or residual binary companion has been observed within the physical extent of the loop to date.

A well resolved image of most SNRs in the optical or UV shows the nebulae taking the form of intertwined sheets, filaments and knots. Recent 850 μm polarimetric observations of Serpens Mains molecular cloud (Kwon et al. 2022) reveal embedded magnetic fields tracing the paths of the filaments – i.e. the filaments glow because the ionized plasma is tied to

the magnetic field! In the context of a SNR, these fields may have been embedded in the ejecta, or could have been compressed by the shock as it rammed in to the ISM. While SNRs provide an opportunity for stellar archaeology, especially of massive stars, whose exothermic lifetimes are comparable to the luminous lifetime of their remnants (i.e. $\sim 10^6$ yr), resolving the progenitor effects from those of the ISM is an as-yet developing science, which relies as much on multi waveband observations as on hydro-dynamic and magneto-hydrodynamic modeling of hot, ionized plasma. A census of galactic SNRs (Green 2019) detected about 300 objects, most of them in the late evolutionary stages, and provides a direct and definitive estimate of the recent supernova rate in the Milky Way galaxy. The well-resolved, nearby, objects are also relatively young ($<$ 10,000 yr), and indicative of the SN-rate in the local galactic region. It is to be noted that although neutron stars are theorized to be born in supernovae (and hence localized with their remnants), there are 50 young pulsars without an associated SNR! Diffusive shock acceleration of the non-thermal tail of electron distribution in the collisionless, forward, shock may also be responsible for Galactic, ultra-high energy cosmic rays ($E = 10^{\sim 14}$ eV), as well as for the synchrotron radiation seen at radio frequencies. The electromagnetic band in which a SNR's luminosity peaks depends on its age. The unique signatures in all parts of the electromagnetic waveband constrain models of late time shock - ISM interaction, as well as (depending on the age, and the presence of a central compact object), provides an insight in to the evolutionary state of the pre-SN progenitor and its CSM. For SNRs that are both optical and X-ray bright, it is important to complement the high temperature (10^{6-7} deg K) phenomena with UV imaging, sampling regions of 10^{4-5} K gas both in the filaments and in other interacting medium.

Since the launch of Astrosat, a new window has opened up in this field – the UV 1300–1800 Å band. This band contains a dense set of diagnostic lines spanning a range of ionization stages, from low-ionization species (e.g. C II, Si II) to higher-ionization resonance lines (e.g., Si IV, C IV), which together trace radiative shocks and post-shock cooling layers in hot gas. The existence of multiple shock fronts, dominated by various ionizaton states, shows the complexity of the local ISM, indicative of intense massive star formation activity in the past.

4 Star Clusters with UV

4.1 Multiple Stellar Populations in Star Clusters

Multiple stellar populations (MPs) in globular and massive clusters manifest as star-to-star variations in He, C, N, O, Na, Al, and sometimes Mg, with classic C–N and O–Na anti-correlations (Carretta et al. 2009; Gratton et al. 2019; Bastian and Lardo 2018). UV filters that cover strong molecular bands (e.g., NH, CN) and crowd metal-line blanketing, notably HST/WFC3 F275W, F336W, and F343N, amplify color differences between first- (1P) and second-population (2P) stars at fixed luminosity (Sbordone et al. 2011; Piotto et al. 2015; Milone et al. 2017). Pseudo-colors such as $C_{\mathrm{F275W,F336W,F438W}}$ or $C_{\mathrm{Un,B,I}}$ map onto nitrogen and helium sensitivity and underpin "chromosome maps," enabling robust photometric tagging from the main sequence (MS) through the red giant branch (RGB) (Milone et al. 2017; Nardiello et al. 2018).

UV-based tagging is particularly powerful where optical color-magnitude diagrams (CMDs) show weak separation. Even modest changes in N and He drive disproportionate UV flux differences for MS, subgiant branch (SGB), and RGB stars, allowing accurate population fractions and radial trends to be measured (Piotto et al. 2015; Dalessandro et al.

2012). Integrated-light UV spectroscopy further ties photometric MPs to abundance patterns in unresolved or distant clusters.

4.2 Rotation, eMSTOs, and UV-Dim Stars

Extended main-sequence turn-offs (eMSTOs) in young and intermediate-age clusters (≤ 2 Gyr) are interpreted as signatures of a distribution of stellar rotation rates rather than age spreads (Bastian and de Mink 2009; Li et al. 2014; Niederhofer et al. 2015; Georgy et al. 2019). Rotation affects internal mixing and stellar lifetimes, leading to broadened MSTOs. UV passbands enhance color shifts, improving contrast between slow and fast rotators (Georgy et al. 2014; Milone et al. 2018; Kamann et al. 2020). The fraction of fast rotators correlates with UV color spreads, supporting rotation as the primary cause of eMSTOs (Milone et al. 2018; Sun et al. 2019; Kamann et al. 2020).

UV-dim stars, which appear redder in UV than in optical bands, may contribute to eMSTOs in young massive clusters. They are thought to have circumstellar disks, with stronger UV absorption by dust causing the UV-dim phenomenon (D'Antona et al. 2023). Fast rotation is suggested to facilitate disk formation, but recent studies indicate that most UV-dim stars are slowly rotating (Leanza et al. 2025). The formation of UV-dim stars may be influenced by their environment, and further research is needed to clarify their origins and correlations with disks, metallicity, or cluster masses.

4.3 UV Bright Population and Binary Products

Ultraviolet observations are indispensable for uncovering the hidden products of binary evolution in clusters, where dense stellar environments foster mass transfer, mergers, and compact remnant formation. While only a few percent of Galactic clusters have UV data, studies already show that UV photometry and spectroscopy uniquely reveal hot companions such as white dwarfs, sdBs, and post-AGB stars that are invisible in the optical. In white dwarf binaries, UV diagnostics constrain cooling ages, progenitor masses, and magnetic or accretion signatures, enabling tests of the initial–final mass relation and binary-interaction channels (Hansen et al. 2007). For blue stragglers, blue lurkers, and yellow stragglers, UV data provide the only direct means to identify mass-transfer histories, bifurcated sequences, and hidden companions, linking observed populations to binary formation pathways (Landsman et al. 1997; Sindhu et al. 2019; Rao et al. 2022). By combining UV sensitivity to hot components with the well-calibrated ages and distances of clusters, these observations yield critical insights into stellar interaction physics, the demographics of exotic stars, and their role in shaping cluster and galaxy evolution.

5 Data in Need

5.1 All-Sky UV Survey

The GALEX surveys covered roughly 60% of the sky ($\approx$24,000 square degrees) while UVIT@AstroSat and UVOT@Swift observations each cover only $\approx$100 square degrees (Roming et al. 2005; Kumar et al. 2012; Bianchi et al. 2017). Most of the unobserved regions lie along the Galactic plane, leaving the UV properties of the majority of Galactic UV sources largely unknown.

A new all-sky ultraviolet (UV) survey is essential because this wavelength regime traces astrophysical processes that are invisible at optical and infrared wavelengths. UV observations provide direct signatures of hot, young, and massive stars, white dwarfs, accreting compact objects, and the diffuse interstellar and circumgalactic medium. Mapping the sky in the UV uniquely reveals star formation histories, stellar populations, and the physics of gas flows that regulate galaxy evolution. While GALEX delivered transformative insights, its incomplete coverage, limited depth, and angular resolution leave significant gaps. A modern, sensitive all-sky UV survey would uncover faint populations, and complement multi-wavelength data. A all-sky survey with a large dynamic range and homogeneous coverage, akin to 2MASS in the near-IR, would provide a foundation for selecting spectroscopic targets, enabling time-domain follow-up, discovering unknown objects, and supporting UV and panchromatic studies for decades to come.

5.2 FUV Spectroscopy

Far-ultraviolet (FUV; 90–200 nm) spectroscopy has proven indispensable for probing stellar photospheres, winds, and circumstellar environments. However, exisiting data remain incomp/lete, hinder our ability to address many fundamental questions in stellar astrophysics. Current knowledge relies predominantly on archival observations from Hubble Space Telescope HST/COS and STIS above 115 nm, with comprehensive sampling limited to only a fraction of stellar types (Green et al. 2012). Coverage below 115 nm, where key resonance lines such as O VI (1032, 1038 Å) and C III (977 Å) reside, is extremely sparse since the loss of Far Ultraviolet Spectroscopic Explorer (FUSE; 1999–2007) (Moos et al. 2000). This significant data deficiency critically impacts constraints on hot-star mass loss, chromospheric heating processes, and the ionizing flux that regulates interstellar and planetary environments (Fullerton et al. 2006).

Critical gaps include: (1) systematic measurements of wind-sensitive resonance lines in massive stars across the full range of metallicities, which are essential to quantify feedback and calibrate stellar evolution models (Massa et al. 2003; Fullerton et al. 2006); (2) time-resolved FUV spectra of cool stars, particularly active M dwarfs, needed to quantify flare-driven variability and its impact on exoplanet atmospheres (France et al. 2012; Loyd et al. 2018); (3) simultaneous FUV coverage of stellar populations in clusters and star-forming regions to establish evolutionary trends and environmental effects (Pineda et al. 2021); and (4) robust empirical connections between observable FUV lines and the unobservable extreme-UV continua of hot stars, which dominate galactic ionization budgets (Heap et al. 2021).

The FUSE facilitated major advances, extending coverage down to 90 nm at $R \sim 20{,}000$, and revealing wind variability and interstellar absorption (Moos et al. 2000). The HST instruments STIS and COS provided sensitive FUV spectroscopy above 115 nm, enabling studies of massive-star winds, stellar flares, and the radiation environments of exoplanet hosts (Green et al. 2012). Low-mass stars, especially M dwarfs, have constituted a major focus. The Far Ultraviolet M-dwarf Evolution Survey (FUMES) established correlations between FUV line luminosities and stellar rotation, showing the decay of high-energy output with age (Pineda et al. 2021). Time-domain observations highlight the importance of flares: comparisons of HST FUV spectra with TESS optical light curves demonstrate that optical-only models underestimate FUV flare energy by orders of magnitude, revealing stars that are "optically quiet but FUV loud". Collectively these findings underscore that direct FUV monitoring is essential to assess exoplanet atmospheric erosion and habitability.

Archival surveys continue to expand our view of stellar populations. HST/COS and STIS spectra have been used to probe massive-star winds and the radiation environments of young

clusters, though coverage remains sparse and often single-epoch. GALEX imaging has also revealed extended FUV structures around evolved stars, tracing circumstellar scattering and shocks. Together, these studies highlight both the vitality of FUV spectroscopy and its limitations: current progress relies heavily on archival HST data, where deficiencies in sensitivity, cadence, and coverage that leave fundamental questions unresolved.

Resolving these open questions demands next-generation FUV spectrographs with high spectral resolution ($R \gtrsim 20{,}000$), large collecting areas, and efficient coverage below 120 nm. Such capabilities would enable precise measurements of massive-star mass-loss rates, systematic mapping of chromospheric heating, and statistical studies of flare-driven FUV variability in M dwarfs. New concepts such as INFUSE, an integral-field unit spectrograph designed for spatially resolved FUV observations of stellar feedback in star-forming regions, illustrate the potential of these future instruments (Haughton et al. 2024). CubeSat-scale efforts, such as SPRITE, aim to provide new access to FUV spectroscopy from small platforms (Bowen et al. 2024). On a large scale, a 6–10 m class UV space telescope would extend FUV spectroscopy to faint stellar populations in the Milky Way and nearby galaxies, advancing models of stellar evolution, feedback, and planetary habitability. While concept studies such as LUVOIR and HabEx, which were later combined into Habitable Worlds Observatory (HWO) (National Academies of Sciences, Engineering, and Medicine 2023), recognized the importance of FUV coverage, realizing these goals depends on breakthroughs in detectors, coatings, and gratings (The LUVOIR Team 2019; Gaudi et al. 2020). Ultimately these fundamental questions can only be resolved with renewed investment in FUV spectroscopy.

5.3 EUV Spectroscopy

Extreme-ultraviolet (EUV; 10–90 nm) spectroscopy provides a unique window into stellar physics, probing continua and resonance lines that directly trace hot atmospheres, stellar coronae, and accretion processes. The EUV contains critical diagnostics such as the He II Lyman series and strong iron lines (Fe IX–Fe XVI), which reveal plasma at 10^5–10^7 K. Despite its importance, EUV spectroscopy has been largely inaccessible since the Extreme Ultraviolet Explorer (EUVE; 1992–2001) (Bowyer 1994), leaving major questions in stellar astrophysics unresolved.

Key open problems requiring EUV spectroscopy include: (1) the detailed photospheric composition and chemical stratification of hot white dwarfs, shaped by diffusion and radiative levitation (Barstow et al. 1997, 2014); (2) the true ionizing continua of hot stars and subdwarfs, where models disagree on the Lyman continuum flux below 912 Å due to uncertain wind opacities (Heap et al. 2021); (3) the mechanisms of stellar coronal heating, whether wave-driven or reconnection-dominated, which can be disentangled only with EUV iron line diagnostics (Linsky et al. 2020); and (4) the impact of stellar EUV radiation on exoplanetary atmospheres, which governs atmospheric escape and habitability (Linsky et al. 2014).

EUVE demonstrated the potential of EUV spectroscopy, producing the first surveys of white dwarfs, active cool stars, and cataclysmic variables. However, its modest collecting area and resolution limited detailed studies, and no successor has been launched. Current FUV and X-ray facilities can only partially address these questions: FUV spectra constrain some transition-region lines, while X-rays probe hotter coronae, but the crucial 10^5–10^6 K plasma and the stellar ionizing continuum remain inaccessible. Roadblocks include high interstellar absorption in the EUV, incomplete atomic data for complex ions, and the technological difficulty of building efficient optics and detectors at short wavelengths.

Resolving these questions requires a new generation of EUV spectrographs with high spectral resolution ($R \gtrsim 10{,}000$) and large collecting areas to overcome interstellar attenuation and capture faint stellar fluxes. Advances in multilayer coatings, grazing-incidence optics, and high-efficiency EUV detectors are essential. A dedicated EUV observatory would enable transformative science: mapping white dwarf abundances, directly measuring stellar ionizing continua, diagnosing coronal heating mechanisms, and quantifying stellar irradiation of exoplanets. Only with renewed access to EUV spectroscopy can these long-standing questions in stellar astrophysics be definitively answered.

5.4 Time-Domain UV

The ultraviolet (UV) domain provides uniquely sensitive diagnostics of stellar variability, tracing phenomena that are often invisible at longer wavelengths. Variability in the UV arises from instabilities in radiatively driven winds, magnetically modulated outflows, accretion shocks in young stars, and flares from cool dwarfs. Because many of the strongest resonance lines (e.g., C IV, N V, Si IV, O VI, Lyα) lie in the UV, even modest fluctuations in density, temperature, or ionization state translate into large changes in spectral line profiles (Fullerton et al. 1996; Martins et al. 2015; Sundqvist and Owocki 2013). Time-resolved UV observations therefore provide direct probes of stellar mass loss, rotation, magnetic fields, and pulsations, as well as the energy input into circumstellar environments and exoplanet atmospheres (France et al. 2016).

Time-resolved UV data thus probe fundamental questions: how structured are OB-star winds and how does this affect mass-loss rates? (Fullerton et al. 1996; Martins et al. 2015) How stochastic is accretion in pre-main-sequence stars? (Gómez de Castro 2013)What is the flare frequency–energy distribution of M dwarfs, and what does this imply for planetary atmospheres (France et al. 2016; Loyd et al. 2018)? And what can early UV light curves of transients such as supernovae or tidal disruption events (TDEs) reveal about stellar structure at the moment of explosion or disruption (Gezari et al. 2012; van Velzen et al. 2021).

Past campaigns with IUE, HST, FUSE, and Swift/UVOT demonstrated the diagnostic power of time-domain UV. Yet these studies are limited to small, heterogeneous samples with sparse cadence, preventing population-level statistics across stellar types. Currently, ULLYSES incorporates multi-epoch monitoring, filling the UV time-domain gap for 250 massive stars with low metallicity (Roman-Duval et al. 2025; Vink et al. 2023). By pairing time-resolved UV with simultaneous X-shooter data, ULLYSES offers the first large, multi-wavelength view of the dynamic lives of massive stars, laying the foundation for interpreting high-redshift galaxy UV spectra with JWST, Roman (Akeson et al. 2019), and Extremely Large Telescopes (ELT; Padovani and Cirasuolo 2023).

The future requires dedicated UV time-domain facilities. ULTRASAT will pioneer wide-field NUV monitoring at minute cadence, enabling flare statistics, wind demographics, and early transient detection (Shvartzvald et al. 2024). Proposed missions such as CETUS (Heap et al. 2021), Polstar (Scowen et al. 2022), CASTOR (Côté et al. 2024), and Pollux (Neiner et al. 2026) would extend capability to FUV spectroscopy, spectropolarimetry, and wide-field surveys, while flagship concepts (such as HWO) promise exquisite time-resolved UV spectroscopy for targeted samples. In parallel, advances in atomic physics and radiation-hydrodynamic modeling are needed to interpret variability signatures robustly.

In short, while time-domain UV studies have revealed the ubiquity of wind variability, stochastic accretion, and energetic flares, the field remains at the case-study stage or limited to small heterogeneous samples. Moving to systematic, population-level surveys with improved atomic data and predictive theory is essential to answer the outstanding questions of stellar mass loss, accretion, magnetism, and disruption.

5.5 Polarimetry in UV

Ultraviole polarimetry represents one of the most powerful yet underutilized and generally neglected frontiers in stellar astrophysics. Because polarization encodes the geometry of scattering and magnetic alignment, UV polarimetric measurements provide a uniquely direct view of asymmetries in stellar atmospheres, winds, and circumstellar environments. Polarization across these lines is sensitive to wind clumping, magnetic channeling, and the imprint of circumstellar structures, offering insights that cannot be obtained from photometry, spectroscopy, or optical polarimetry alone (Kasen et al. 2003; Ignace et al. 2015).

How do massive stars lose mass through radiatively driven winds? What role do magnetic fields play in shaping these outflows and channeling material? How do disks around young stars and compact binaries evolve under intense UV radiation? UV polarimetry addresses these questions by measuring continuum and line polarization, sensitive to clumping, magnetic confinement, and disk geometry. Resonance lines such as C IV, Si IV, and N V are especially valuable, since their polarized line profiles encode information about wind geometry and variability (Kasen et al. 2003; Ignace et al. 2015).

Despite this potential, the development of UV polarimetry has lagged far behind other techniques. The Wisconsin Ultraviolet Photo-Polarimeter Experiment (WUPE), flown in 1990, remains the only space-based mission dedicated to UV polarimetry (Stanford et al. 1985). Subsequent UV observatories, including HST and FUSE, lacked polarimetric capability, leaving the field effectively dormant for more than three decades. This gap has severely constrained progress: while optical and infrared polarimetry have revolutionized studies of magnetic fields, disks, and dust, the most energetic stellar environments—where mass loss, feedback, and accretion are governed by UV radiation—remain beyond reach. The absence of UV polarimetry is thus a fundamental limitation in our ability to trace the flow of mass and energy from stars into the interstellar medium.

The challenges are primarily technological. Efficient polarization optics are difficult to implement at short wavelengths, where birefringent materials become inefficient and transparent choices are limited largely to MgF_2, which restricts bandwidth and achromatic design (Keller et al. 1998; Neiner et al. 2025). At still shorter UV wavelengths, transmissive retarders vanish entirely and one must rely on reflective or thin-film polarizers, which suffer reduced efficiency and polarization purity (Keller et al. 1998). Wave retarders in the UV can also act as weak polarizers, introducing unwanted instrumental effects that complicate calibration. Calibration itself is especially demanding: coatings, gratings, and mirrors can all introduce significant polarization systematics, requiring full Mueller-matrix characterization to achieve accuracy at the sub-percent level (Chipman et al. 2015). Moreover, stellar UV fluxes are intrinsically low, necessitating large collecting areas and high-throughput instrumentation to reach adequate signal-to-noise (Chipman et al. 2015). Overcoming these hurdles will demand innovations in detector technology, careful polarimetric design, and sustained attention to calibration strategies.

Momentum is now building toward a revival of the field. For example, the proposed PolStar MIDEX mission was conceived as a dedicated far-UV spectropolarimeter (100–300 nm), targeting massive star winds, magnetospheres, and circumstellar disks (Scowen et al. 2022). Another proposed mission, URIEL (Ultraviolet Researcher to Investigate the Emergence of Life) is designed to carry out low dispersion (600–1,000) UV /spectropolarimetry in the 140-400 nm spectral range to investigate the formation of planetary systems, its interaction with stellar winds and search for signatures of prebiotic molecules (Gómez de Castro et al. 2022). On longer timescales, future missions, such as PolStar, Arago (Muslimov and Neiner 2022), and Pollux onboard the flagship HWO, will provide UV–optical–IR polarimetric capabilities that would enable population-level studies across stellar

types and environments. If realized, these missions could capture not only static geometries but also time-dependent signatures, such as rotational modulation, binary interactions, and flares, connecting UV polarization with stellar dynamics on multiple timescales.

In conclusion, UV polarimetry offers transformative potential for stellar astrophysics, with the ability to directly constrain mass loss, magnetic confinement, and circumstellar structure in the UV-dominated regime where these processes are most active. Yet this potential has scarcely been realized, with the last dedicated measurements now over thirty years old. The primary barriers are instrumental, not scientific. Investment in dedicated polarimetric capability on future UV missions would therefore open an entirely new window on stellar physics, addressing some of the most persistent questions about how stars interact with and shape their environments.

Acknowledgements GDZ acknowledges support from STFC (UK) via the consolidated grant to the atomic astrophysics group at DAMTP, University of Cambridge (ST/T000481/1) and the STFC large Award UKRI1165: the Solar Atmospheric modelling Suite (SAMS). XF acknowledges the support of the National Natural Science Foundation of China (NSFC) No. 12573040, No. 12533008, and No. 12203100. VVJ acknowledges support through grant 26-217745 from the Czech Grant Agency.

Declarations

Competing Interests The authors declare no competing interests.

Open Access This article is licensed under a Creative Commons Attribution 4.0 International License, which permits use, sharing, adaptation, distribution and reproduction in any medium or format, as long as you give appropriate credit to the original author(s) and the source, provide a link to the Creative Commons licence, and indicate if changes were made. The images or other third party material in this article are included in the article's Creative Commons licence, unless indicated otherwise in a credit line to the material. If material is not included in the article's Creative Commons licence and your intended use is not permitted by statutory regulation or exceeds the permitted use, you will need to obtain permission directly from the copyright holder. To view a copy of this licence, visit http://creativecommons.org/licenses/by/4.0/.

References

Akeson R, Armus L, Bachelet E, et al (2019) The Wide Field Infrared Survey Telescope: 100 Hubbles for the 2020s. arXiv e-prints arXiv:1902.05569. https://doi.org/10.48550/arXiv.1902.05569

Amarsi AM, Asplund M, Collet R, et al (2016) Non-LTE oxygen line formation in 3D hydrodynamic model stellar atmospheres. Mon Not R Astron Soc 455(4):3735–3751. https://doi.org/10.1093/mnras/stv2608. arXiv:1511.01155 [astro-ph.SR]

Asplund M, Amarsi AM, Grevesse N (2021) The chemical make-up of the Sun: a 2020 vision. Astron Astrophys 653:A141. https://doi.org/10.1051/0004-6361/202140445. arXiv:2105.01661 [astro-ph.SR]

Ayres TR (2015) The far-ultraviolet ups and downs of Alpha Centauri. Astron J 149:58. https://doi.org/10.1088/0004-6256/149/2/58

Ayres TR, Marstad NC, Linsky JL (1981) Outer atmospheres of cool stars. IX. A survey of ultraviolet emission from F-K dwarfs and giants with the IUE. Astrophys J 247:545–559. https://doi.org/10.1086/159065

Badenes C, Maoz D, Ciardullo R (2015) The progenitors and lifetimes of planetary nebulae. Astrophys J 804(1):L25. https://doi.org/10.1088/2041-8205/804/1/L25. arXiv:1502.01015 [astro-ph.SR]

Badnell NR (2006) Radiative recombination data for modeling dynamic finite-density plasmas. Astrophys J Suppl Ser 167:334–342. https://doi.org/10.1086/508465

Badnell NR, O'Mullane MG, Summers HP, et al (2003) Dielectronic recombination data for dynamic finite-density plasmas. I. Goals and methodology. Astron Astrophys 406:1151–1165. https://doi.org/10.1051/0004-6361:20030816

Barstow MA, Dobbie PD, Holberg JB, et al (1997) Interstellar and photospheric opacity from EUV spectroscopy of DA white dwarfs. Mon Not R Astron Soc 286(1):58–76. https://doi.org/10.1093/mnras/286.1.58

Barstow MA, Barstow JK, Casewell SL, et al (2014) Evidence for an external origin of heavy elements in hot DA white dwarfs. Mon Not R Astron Soc 440(2):1607–1625. https://doi.org/10.1093/mnras/stu216. arXiv:1402.2164 [astro-ph.SR]

Barstow MA, Battisti A, Favata F, et al (2026) UV astronomical facilities for the 21st century. Space Sci Rev 222

Baschek B, Kudritzki RP, Scholz M (1980) The far ultraviolet spectrum of the B-type subdwarf HD 205805. In: Battrick B, Mort J (eds) Ultraviolet observations of Quasars, pp 319–322

Bastian N, de Mink SE (2009) The effect of stellar rotation on colour-magnitude diagrams: on the apparent presence of multiple populations in intermediate age stellar clusters. Mon Not R Astron Soc 398(1):L11–L15. https://doi.org/10.1111/j.1745-3933.2009.00696.x. arXiv:0906.1590 [astro-ph.GA]

Bastian N, Lardo C (2018) Multiple stellar populations in globular clusters. Annu Rev Astron Astrophys 56:83–136. https://doi.org/10.1146/annurev-astro-081817-051839. arXiv:1712.01286 [astro-ph.SR]

Battich T, Miller Bertolami MM, Weiss A, et al (2025) The I-processes nucleosynthesis during the formation of He-rich hot-subdwarf stars. Astron Astrophys 699:A298. https://doi.org/10.1051/0004-6361/202453572. arXiv:2503.23541 [astro-ph.SR]

Bhattacharya S, Arnaboldi M, Caldwell N, et al (2019) The survey of planetary nebulae in Andromeda (M 31). II. Age-velocity dispersion relation in the disc from planetary nebulae. Astron Astrophys 631:A56. https://doi.org/10.1051/0004-6361/201935898. arXiv:1909.09724 [astro-ph.GA]

Bianchi L, Shiao B, Thilker D (2017) Revised catalog of GALEX ultraviolet sources. I. The all-sky survey: GUVcat_AIS. Astrophys J Suppl Ser 230(2):24. https://doi.org/10.3847/1538-4365/aa7053. arXiv:1704.05903 [astro-ph.GA]

Boggess A, Carr FA, Evans DC, et al (1978) The IUE spacecraft and instrumentation. Nature 275:372–377. https://doi.org/10.1038/275372a0

Bowen M, Fleming B, Indahl B, et al (2024) Preflight characterization of the SPRITE CubeSat: a far-UV imaging spectrograph for stellar feedback in local galaxies. In: den Herder JWA, Nikzad S, Nakazawa K (eds) Space telescopes and instrumentation 2024: ultraviolet to gamma ray, p 1309334. https://doi.org/10.1117/12.3020453

Bowyer S (1994) Astronomy and the extreme ultraviolet explorer satellite. Science 263(5143):55–59. https://doi.org/10.1126/science.11536659

Bowyer S, Malina RF (1991) The extreme ultraviolet explorer mission. Adv Space Res 11(11):11–18. https://doi.org/10.1016/0273-1177(91)90077-W

Brandt JC, Heap SR, Beaver EA, et al (1994) The Goddard high resolution spectrograph: instrument, goals, and science results. Publ Astron Soc Pac 106:890. https://doi.org/10.1086/133457

Brosch N, Almoznino E, Leibowitz EM, et al (1995) A study of ultraviolet objects near the North galactic pole with FAUST. Astrophys J 450:137. https://doi.org/10.1086/176125

Brose R, Pohl M, Sushch I (2021) Morphology of supernova remnants and their halos. Astron Astrophys 654:A139. https://doi.org/10.1051/0004-6361/202141194

Burgess A (1964) Delectronic recombination and the temperature of the solar corona. Astrophys J 139:776–780. https://doi.org/10.1086/147813

Calvet N, Gullbring E (1998) The structure and emission of the accretion shock in T Tauri Stars. Astrophys J 509(2):802–818. https://doi.org/10.1086/306527

Carlsson M (1986) A computer program for solving multi-level non-LTE radiative transferproblems in moving or static atmospheres. Uppsala Astronomical Observatory Reports 33

Carnochan DJ, Wilson R (1983) A survey of ultraviolet objects. Mon Not R Astron Soc 202:317–345. https://doi.org/10.1093/mnras/202.2.317

Carnochan DJ, Dworetsky MM, Todd JJ, et al (1975) A search for ultraviolet objects. Philos Trans R Soc Lond Ser A 279(1289):479–485. https://doi.org/10.1098/rsta.1975.0084

Carretta E, Bragaglia A, Gratton RG, et al (2009) Na-O anticorrelation and HB. VII. The chemical composition of first and second-generation stars in 15 globular clusters from GIRAFFE spectra. Astron Astrophys 505(1):117–138. https://doi.org/10.1051/0004-6361/200912096. arXiv:0909.2938 [astro-ph.GA]

Castor JI, Abbott DC, Klein RI (1975) Radiation-driven winds in Of stars. Astrophys J 195:157–174. https://doi.org/10.1086/153315

Chayer P, Dixon W (2014) Spectroscopic analysis of hot subdwarf stars in the globular cluster NGC 6752. In: van Grootel V, Green E, Fontaine G, et al (eds) 6th meeting on hot subdwarf stars and related objects, p 59

Chevalier RA (1977) The interaction of supernovae with the interstellar medium. Annu Rev Astron Astrophys 15:175–196. https://doi.org/10.1146/annurev.aa.15.090177.001135

Chipman RA, Lam WST, Breckinridge J (2015) Polarization aberration in astronomical telescopes. In: Shaw JA, LeMaster DA (eds) Polarization science and remote sensing VII, p 96130H. https://doi.org/10.1117/12.2188921

Côté P, Amenouche M, Lokhorst D (2024) Design and status of the CASTOR mission. In: den Herder JWA, Nikzad S, Nakazawa K (eds) Space telescopes and instrumentation 2024: ultraviolet to gamma ray, p 130933A. https://doi.org/10.1117/12.3019209

Dalessandro E, Schiavon RP, Rood RT, et al (2012) Ultraviolet properties of galactic globular clusters with galex. II. Integrated colors. Astron J 144(5):126. https://doi.org/10.1088/0004-6256/144/5/126. arXiv:1208.5698 [astro-ph.GA]

D'Antona F, Dell'Agli F, Tailo M, et al (2023) On the role of dust and mass-loss in the extended main sequence turnoff of star clusters: the case of NGC 1783. Mon Not R Astron Soc 521(3):4462–4472. https://doi.org/10.1093/mnras/stad851. arXiv:2303.16049 [astro-ph.SR]

Dawson H, Geier S, Heber U, et al (2024) A 500 pc volume-limited sample of hot subluminous stars. I. Space density, scale height, and population properties. Astron Astrophys 686:A25. https://doi.org/10.1051/0004-6361/202348319. arXiv:2403.15513 [astro-ph.SR]

De Marco O (2009) The origin and shaping of planetary nebulae: putting the binary hypothesis to the test. Publ Astron Soc Pac 121(878):316. https://doi.org/10.1086/597765. arXiv:0902.1137 [astro-ph.GA]

De Pasquale M, Schady P, Kuin NPM, et al (2010) Swift and Fermi observations of the early afterglow of the short gamma-ray burst 090510. Astrophys J 709(2):L146–L151. https://doi.org/10.1088/2041-8205/709/2/L146. arXiv:0910.1629 [astro-ph.HE]

Del Zanna G (2012) Benchmarking atomic data for astrophysics: a first look at the soft X-ray lines. Astron Astrophys 546:A97. https://doi.org/10.1051/0004-6361/201219923

Del Zanna G, Andretta V (2015) The EUV spectrum of the Sun: irradiances during 1998-2014. Astron Astrophys 584:A29. https://doi.org/10.1051/0004-6361/201526804

Del Zanna G, Mason HE (2018) Solar UV and X-ray spectral diagnostics. Living Rev Sol Phys 15:5. https://doi.org/10.1007/s41116-018-0015-3

Del Zanna G, Landini M, Mason HE (2002) Spectroscopic diagnostics of stellar transition regions and coronae in the XUV: AU Mic in quiescence. Astron Astrophys 385:968–985. https://doi.org/10.1051/0004-6361:20020164

Del Zanna G, Storey PJ, Badnell NR, et al (2020) Helium line emissivities in the solar corona. Astrophys J 898(1):72. https://doi.org/10.3847/1538-4357/ab9d84

Del Zanna G, Dere KP, Young PR, et al (2021) CHIANTI—an atomic database for emission lines. XVI. Version 10, further extensions. Astrophys J 909(1):38. https://doi.org/10.3847/1538-4357/abd8ce

Del Zanna G, Liang G, Mao J, et al (2025a) UK APAP R-matrix electron-impact excitation cross-sections for modelling laboratory and astrophysical plasma. Atoms 13(5):44. https://doi.org/10.3390/atoms13050044

Del Zanna G, Mason HE, Storey PJ, et al (2025b) Nigel R. Badnell (1958-2024): a legacy in atomic astrophysics. Atoms 13(6):55. https://doi.org/10.3390/atoms13060055

Deliporanidou E, Del Zanna G (2024) Modelling stellar irradiances I: the transition regions of FGKM stars. Mon Not R Astron Soc 534(4):3989–3998. https://doi.org/10.1093/mnras/stae2299

Deliporanidou E, Del Zanna G, Woods TN, et al (2025) Modelling stellar irradiances – II. Correlations of solar irradiances with proxies of activity along a cycle. Mon Not R Astron Soc 540(2):1765–1779. https://doi.org/10.1093/mnras/staf812

Dopita MA, Meatheringham SJ (1991) Photoionization modeling of magellanic cloud planetary nebulae. I. Astrophys J 367:115. https://doi.org/10.1086/169607

Dorsch M, Latour M, Heber U (2019) Heavy metals in intermediate He-rich hot subdwarfs: the chemical composition of HZ 44 and HD 127493. Astron Astrophys 630:A130. https://doi.org/10.1051/0004-6361/201935724. arXiv:1907.07781 [astro-ph.SR]

Dorsch M, Jeffery CS, Irrgang A, et al (2021) EC 22536-5304: a lead-rich and metal-poor long-period binary. Astron Astrophys 653:A120. https://doi.org/10.1051/0004-6361/202141381. arXiv:2107.06340 [astro-ph.SR]

Drew JE, Greimel R, Irwin MJ, et al (2005) The INT Photometric Hα Survey of the Northern Galactic Plane (IPHAS). Mon Not R Astron Soc 362(3):753–776. https://doi.org/10.1111/j.1365-2966.2005.09330.x. arXiv:astro-ph/0506726 [astro-ph]

Drew JE, Gonzalez-Solares E, Greimel R, et al (2014) The VST Photometric Hα Survey of the Southern Galactic Plane and Bulge (VPHAS+). Mon Not R Astron Soc 440(3):2036–2058. https://doi.org/10.1093/mnras/stu394. arXiv:1402.7024 [astro-ph.GA]

Drout MR, Götberg Y, Ludwig BA, et al (2023) An observed population of intermediate-mass helium stars that have been stripped in binaries. Science 382(6676):1287–1291. https://doi.org/10.1126/science.ade4970. arXiv:2307.00061 [astro-ph.SR]

Dufresne RP, Del Zanna G (2026) Level-resolved photoionization cross-sections for modelling astrophysical plasma Mon Not R Astron Soc 546(4) https://doi.org/10.1093/mnras/stag239

Dufresne RP, Del Zanna G, Young PR, et al (2024) CHIANTI—an atomic database for emission lines—paper. XVIII. Version 11, advanced ionization equilibrium models: density and charge transfer effects. Astrophys J 974(1):71. https://doi.org/10.3847/1538-4357/ad6765

Dufresne RP, Del Zanna G, Osborne CMJ (2026) Diagnostics for the solar chromosphere using neutral carbon Rydberg lines. Mon Not R Astron Soc 546(2):stag076. https://doi.org/10.1093/mnras/stag076
Dufresne RP, Del Zanna G, Osborne CMJ (2025) Improving the atomic modelling for solar UV radiative transfer calculations. Mon Not R Astron Soc 542(3):2223–2237. https://doi.org/10.1093/mnras/staf1330
Fesen RA, Weil KE, Cisneros IA, et al (2018) The Cygnus Loop's distance, properties, and environment driven morphology. Mon Not R Astron Soc 481(2):1786–1798. https://doi.org/10.1093/mnras/sty2370. arXiv:1809.01713 [astro-ph.HE]
Fesen RA, Drechsler M, Weil KE, et al (2021) Far-UV and optical emissions from three very large supernova remnants located at unusually high galactic latitudes. Astrophys J 920(2):90. https://doi.org/10.3847/1538-4357/ac0ada
Fontenla JM, Avrett EH, Loeser R (1990) Energy balance in the solar transition region. I. Hydrostatic thermal models with ambipolar diffusion. Astrophys J 355:700. https://doi.org/10.1086/168803
Fontenla JM, Landi E, Snow M, et al (2014) Far- and extreme-UV solar spectral irradiance and radiance from simplified atmospheric physical models. Sol Phys 289(2):515–544. https://doi.org/10.1007/s11207-013-0431-4
Ford HC, Clampin M, Hartig GF, et al (2003) Overview of the advanced camera for surveys on-orbit performance. In: Blades JC, Siegmund OHW (eds) Future EUV/UV and visible space astrophysics missions and instrumentation, pp 81–94. https://doi.org/10.1117/12.460040
France K, Linsky JL, Tian F, et al (2012) The ultraviolet radiation environment around m dwarf exoplanet host stars. Astrophys J 750:L32. https://doi.org/10.1088/2041-8205/750/2/L32
France K, Loyd ROP, Youngblood A, et al (2016) The muscles treasury survey. I. Motivation and overview. Astrophys J 820(2):89. https://doi.org/10.3847/0004-637X/820/2/89
Frew DJ, Parker QA (2010) Planetary nebulae: observational properties, mimics and diagnostics. Publ Astron Soc Aust 27(2):129–148. https://doi.org/10.1071/AS09040. arXiv:1002.1525 [astro-ph.SR]
Frew DJ, Parker QA, Bojičić IS (2016) The Hα surface brightness-radius relation: a robust statistical distance indicator for planetary nebulae. Mon Not R Astron Soc 455(2):1459–1488. https://doi.org/10.1093/mnras/stv1516. arXiv:1504.01534 [astro-ph.SR]
Froese Fischer C, Tachiev G, Gaigalas G, et al (2007) An MCHF atomic-structure package for large-scale calculations. Comput Phys Commun 176(8):559–579. https://doi.org/10.1016/j.cpc.2007.01.006
Fullerton AW, Gies DR, Bolton CT (1996) Absorption line profile variations among the O stars. I. The incidence of variability. Astrophys J Suppl Ser 103:475. https://doi.org/10.1086/192285
Fullerton AW, Massa DL, Prinja RK (2006) The discordance of mass-loss estimates for o-type stars. Astrophys J 637:1025–1039. https://doi.org/10.1086/498560
Gardner JP, Mather JC, Abbott R, et al (2023) The James Webb Space Telescope mission. Publ Astron Soc Pac 135(1048):068001. https://doi.org/10.1088/1538-3873/acd1b5. arXiv:2304.04869 [astro-ph.IM]
Gaudi BS, et al (2020) The habitable exoplanet observatory (HabEx) mission concept study final report. arXiv:2001.06683
Gehrels N, Chincarini G, Giommi P, et al (2004) The Swift gamma-ray burst mission. Astrophys J 611(2):1005–1020. https://doi.org/10.1086/422091. arXiv:astro-ph/0405233 [astro-ph]
Geier S, Raddi R, Gentile Fusillo NP, et al (2019) The population of hot subdwarf stars studied with Gaia. II. The Gaia DR2 catalogue of hot subluminous stars. Astron Astrophys 621:A38. https://doi.org/10.1051/0004-6361/201834236. arXiv:1810.09321 [astro-ph.SR]
Geier S, Heber U, Irrgang A, et al (2024) A spectroscopic and kinematic survey of fast hot subdwarfs. Astron Astrophys 690:A368. https://doi.org/10.1051/0004-6361/202450778. arXiv:2407.04479 [astro-ph.SR]
Georgy C, Granada A, Ekström S, et al (2014) Populations of rotating stars. III. SYCLIST, the new Geneva population synthesis code. Astron Astrophys 566:A21. https://doi.org/10.1051/0004-6361/201423881. arXiv:1404.6952 [astro-ph.SR]
Georgy C, Charbonnel C, Amard L, et al (2019) Disappearance of the extended main sequence turn-off in intermediate age clusters as a consequence of magnetic braking. Astron Astrophys 622:A66. https://doi.org/10.1051/0004-6361/201834505. arXiv:1812.05544 [astro-ph.SR]
Gesicki K, Zijlstra AA (2000) Expansion velocities and dynamical ages of planetary nebulae. Astron Astrophys 358:1058–1068
Gezari S, Chornock R, Rest A, et al (2012) An ultraviolet-optical flare from the tidal disruption of a helium-rich stellar core. Nature 485(7397):217–220. https://doi.org/10.1038/nature10990. arXiv:1205.0252 [astro-ph.CO]
Gies DR, Bagnuolo WG Jr, Ferrara EC, et al (1998) Hubble Space Telescope Goddard High Resolution Spectrograph Observations of the Be + sdO Binary φ Persei. Astrophys J 493(1):440–450. https://doi.org/10.1086/305113
Gómez de Castro AI (2013) Young stellar objects and protostellar disks. In: Oswalt TD, Barstow MA (eds) Planets, stars and stellar systems. Volume 4: stellar structure and evolution. Springer, Dordrecht, p 279. https://doi.org/10.1007/978-94-007-5615-1_6

Gómez de Castro AI, de Isidro-Gómez AI, de Leyva D, et al (2022) The ultraviolet researcher to investigate the emergence of life: a mission proposal to ESA's F-call. In: den Herder JWA, Nikzad S, Nakazawa K (eds) Space telescopes and instrumentation 2022: ultraviolet to gamma ray, p 121810E. https://doi.org/10.1117/12.2630650

Grant IP, McKenzie BJ, Norrington PH, et al (1980) An atomic multiconfigurational Dirac-Fock package. Comput Phys Commun 21(2):207–231. https://doi.org/10.1016/0010-4655(80)90041-7

Gratton R, Bragaglia A, Carretta E, et al (2019) What is a globular cluster? An observational perspective. Astron Astrophys Rev 27(1):8. https://doi.org/10.1007/s00159-019-0119-3. arXiv:1911.02835 [astro-ph.SR]

Green DA (2019) A revised catalogue of 294 galactic supernova remnants. J Astrophys Astron 40(4):36. https://doi.org/10.1007/s12036-019-9601-6. arXiv:1907.02638 [astro-ph.GA]

Green JC, Froning CS, Osterman S, et al (2012) The cosmic origins spectrograph. Astrophys J 744(1):60. https://doi.org/10.1088/0004-637X/744/1/60

Gudiksen BV, Carlsson M, Hansteen VH, et al (2011) The stellar atmosphere simulation code Bifrost. Code description and validation. Astron Astrophys 531:A154. https://doi.org/10.1051/0004-6361/201116520. arXiv:1105.6306 [astro-ph.SR]

Haardt F, Madau P (1996) Radiative transfer in a clumpy universe. II. The ultraviolet extragalactic background. Astrophys J 461:20. https://doi.org/10.1086/177035. arXiv:astro-ph/9509093 [astro-ph]

Haardt F, Madau P (2012) Radiative transfer in a clumpy universe. IV. New synthesis models of the cosmic UV/X-ray background. Astrophys J 746(2):125. https://doi.org/10.1088/0004-637X/746/2/125

Haberreiter M, Delouille V, Mampaey B, et al (2014) Reconstruction of the solar EUV irradiance from 1996 to 2010 based on SOHO/EIT images. J Space Weather Space Clim 4:A30. https://doi.org/10.1051/swsc/2014027

Hall JC (2008) Stellar chromospheric activity. Living Rev Sol Phys 5:2. https://doi.org/10.12942/lrsp-2008-2

Hamann WR, Gruschinske J, Kudritzki RP, et al (1981) Mass loss from O subdwarfs. Astron Astrophys 104:249–255

Hansen BMS, Anderson J, Brewer J, et al (2007) The white dwarf cooling sequence of NGC 6397. Astrophys J 671(1):380–401. https://doi.org/10.1086/522567. arXiv:astro-ph/0701738 [astro-ph]

Harms R, Fitch J (1991) Faint object spectrograph early performance. In: Bely PY, Breckinridge JB (eds) Space astronomical telescopes and instruments, pp 49–65. https://doi.org/10.1117/12.46713

Haughton A, Witt EM, Fleming BT, et al (2024) INFUSE: inflight performance and future improvements for the first FUV integral field spectrograph to study the influence of massive stars on galaxies. In: den Herder JWA, Nikzad S, Nakazawa K (eds) Space telescopes and instrumentation 2024: ultraviolet to gamma ray, p 1309307. https://doi.org/10.1117/12.3020195

Heap SR, Boggess A, Holm A, et al (1978) IUE observations of hot stars: HZ 43, BD +75 325, NGC 6826, SS Cyg, eta Car. Nature 275:385–388. https://doi.org/10.1038/275385a0

Heap SR, Fleming B, Hull T, et al (2021) Progress report on the NASA probe mission concept, CETUS. In: den Herder JWA, Nikzad S, Nakazawa K (eds) Space telescopes and instrumentation 2020: ultraviolet to gamma ray, p 1144408. https://doi.org/10.1117/12.2562715

Heber U (2016) Hot subluminous stars. Publ Astron Soc Pac 128(966):082001. https://doi.org/10.1088/1538-3873/128/966/082001. arXiv:1604.07749 [astro-ph.SR]

Heber U, Hunger K, Jonas G, et al (1984) The atmosphere of sublumious B stars. Astron Astrophys 130:119–130

Hillwig TC, Jones D, De Marco O, et al (2016) Observational confirmation of a link between common envelope binary interaction and planetary nebula shaping. Astrophys J 832(2):125. https://doi.org/10.3847/0004-637X/832/2/125. arXiv:1609.02185 [astro-ph.SR]

Hollenbach DJ, Tielens AGGM (1999) Photodissociation regions in the interstellar medium of galaxies. Rev Mod Phys 71(1):173–230. https://doi.org/10.1103/RevModPhys.71.173

Hubeny I (1997) Stellar atmospheres theory: an introduction. In: De Greve JP, Blomme R, Hensberge H (eds) Stellar atmospheres: theory and observations. Lecture Notes in Physics, vol 497. Springer, Berlin, pp 1–68 https://doi.org/10.1007/BFb0113481

Hubeny I, Lanz T (1995) Non-LTE line-blanketed model atmospheres of hot stars. I. Hybrid complete linearization/accelerated lambda iteration method. Astrophys J 439:875. https://doi.org/10.1086/175226

Hubeny I, Mihalas D (2015) Theory of stellar atmospheres. An introduction to astrophysical non-equilibrium quantitative spectroscopic analysis. Princeton University Press, Princeton

Humason ML, Zwicky F (1947) A search for faint blue stars. Astrophys J 105:85. https://doi.org/10.1086/144884

Hummer DG, Storey PJ (1987) Recombination-line intensities for hydrogenic ions - I. Case B calculations for H I and He II. Mon Not R Astron Soc 224:801–820. https://doi.org/10.1093/mnras/224.3.801

Ignace R, St-Louis N, Proulx-Giraldeau F (2015) Polarimetric modeling of corotating interaction regions threading massive-star winds. Astron Astrophys 575:A129. https://doi.org/10.1051/0004-6361/201424806. arXiv:1501.07563 [astro-ph.SR]

Jones A, Noll S, Kausch W, et al (2013) An advanced scattered moonlight model for Cerro Paranal. Astron Astrophys 560:A91. https://doi.org/10.1051/0004-6361/201322433. arXiv:1310.7030 [astro-ph.IM]
Kalkofen W (2012) The validity of dynamical models of the solar atmosphere. Sol Phys 276(1–2):75–95. https://doi.org/10.1007/s11207-011-9898-z
Kamann S, Bastian N, Gossage S, et al (2020) How stellar rotation shapes the colour-magnitude diagram of the massive intermediate-age star cluster NGC 1846. Mon Not R Astron Soc 492(2):2177–2192. https://doi.org/10.1093/mnras/stz3583. arXiv:2001.01731 [astro-ph.SR]
Kasen D, Nugent P, Wang L, et al (2003) Analysis of the flux and polarization spectra of the type Ia supernova SN 2001el: exploring the geometry of the high-velocity ejecta. Astrophys J 593(2):788–808. https://doi.org/10.1086/376601. arXiv:astro-ph/0301312 [astro-ph]
Keller CU, Plymate C, Ammons SM (1998) Polarization properties of optical elements at uv wavelengths. In: NASA technical report. https://ntrs.nasa.gov/api/citations/19980031492/downloads/19980031492.pdf
Koralesky B, Rudnick L, Gotthelf EV, et al (1998) The X-ray expansion of the supernova remnant Cassiopeia A. Astrophys J 505(1):L27–L30. https://doi.org/10.1086/311604. arXiv:astro-ph/9806241 [astro-ph]
Kudritzki RP, Puls J (2000) Winds from hot stars. Annu Rev Astron Astrophys 38:613–666. https://doi.org/10.1146/annurev.astro.38.1.613
Kumar A, Ghosh SK, Hutchings J, et al (2012) Ultra Violet Imaging Telescope (UVIT) on ASTROSAT. In: Takahashi T, Murray SS, den Herder JWA (eds) Space telescopes and instrumentation 2012: ultraviolet to gamma ray, p 84431N. https://doi.org/10.1117/12.924507. arXiv:1208.4670
Kwitter KB, Henry RBC (2022) Planetary nebulae: sources of enlightenment. Publ Astron Soc Pac 134(1032):022001. https://doi.org/10.1088/1538-3873/ac32b1. arXiv:2110.13993 [astro-ph.SR]
Kwon W, Pattle K, Sadavoy S, et al (2022) B-fields in Star-forming Region Observations (BISTRO): magnetic fields in the filamentary structures of serpens main. Astrophys J 926(2):163. https://doi.org/10.3847/1538-4357/ac4bbe. arXiv:2201.05059 [astro-ph.GA]
Laget M, Vuillemin A, Parsons SB, et al (1978) A hot subluminous star: HDE 283048. Astrophys J 219:165–167. https://doi.org/10.1086/155765
Laming JM (2015) The FIP and inverse FIP effects in solar and stellar coronae. Living Rev Sol Phys 12:2. https://doi.org/10.1007/lrsp-2015-2
Lamontagne R, Wesemael F, Fontaine G, et al (1985) Studies of hot B subdwarfs. III. Carbon, nitrogen and silicon abundances in three sdB stars. Astrophys J 299:496–504. https://doi.org/10.1086/163716
Landsman W, Aparicio J, Bergeron P, et al (1997) S1040 in M67: a post–mass transfer binary with a helium core white dwarf. Astrophys J 481(2):L93–L96. https://doi.org/10.1086/310654. arXiv:astro-ph/9703053 [astro-ph]
Landstorfer A, Rauch T, Werner K (2024) Spectral analysis of three hot subdwarf stars: EC 11481-2303, Feige 110, and PG 0909+276. A critical oscillator-strength evaluation for iron-group elements. Astron Astrophys 688:A101. https://doi.org/10.1051/0004-6361/202450695. arXiv:2406.13307 [astro-ph.SR]
Lanz T, Hubeny I (2007) A grid of NLTE line-blanketed model atmospheres of early B-type stars. Astrophys J Suppl Ser 169(1):83–104. https://doi.org/10.1086/511270. arXiv:astro-ph/0611891 [astro-ph]
Lanz T, Hubeny I, Heap SR (1997) Non-LTE line-blanketed model atmospheres of hot stars. III. Hot subdwarfs: the sdO star BD +75°325. Astrophys J 485(2):843–858. https://doi.org/10.1086/304455
Latour M, Randall SK, Chayer P, et al (2017) Just how hot are the ω Centauri extreme horizontal branch pulsators? Astron Astrophys 600:A130. https://doi.org/10.1051/0004-6361/201630132. arXiv:1702.07609 [astro-ph.SR]
Leanza S, Dalessandro E, Cadelano M, et al (2025) Stellar rotation in the intermediate-age massive cluster NGC 1783: clues about the nature of UV-dim stars. Astron Astrophys 698:A27. https://doi.org/10.1051/0004-6361/202553956. arXiv:2504.08362 [astro-ph.GA]
Leenaarts J (2020) Radiation hydrodynamics in simulations of the solar atmosphere. Living Rev Sol Phys 17(1):3. https://doi.org/10.1007/s41116-020-0024-x
Li C, de Grijs R, Deng L (2014) The exclusion of a significant range of ages in a massive star cluster. Nature 516(7531):367–369. https://doi.org/10.1038/nature13969. arXiv:1412.5368 [astro-ph.SR]
Lin HH, Carlsson M (2015) The formation of iris diagnostics. VII. The formation of the o i 135.56 nm line in the solar atmosphere. Astrophys J 813(1):34. https://doi.org/10.1088/0004-637X/813/1/34
Lin HH, Carlsson M, Leenaarts J (2017) The formation of IRIS diagnostics. IX. The formation of the C I 135.58 NM line in the solar atmosphere. Astrophys J 846(1):40. https://doi.org/10.3847/1538-4357/aa8458
Linsky J (2019) Host stars and their effects on exoplanet atmospheres. Lecture notes in physics, vol 955. Springer, Berlin. https://doi.org/10.1007/978-3-030-11452-7
Linsky JL, Fontenla J, France K (2014) The intrinsic extreme ultraviolet fluxes of F5 V to M5 V stars. Astrophys J 780:61. https://doi.org/10.1088/0004-637X/780/1/61
Linsky JL, Wood BE, Youngblood A, et al (2020) The relative emission from chromospheres and coronae: dependence on spectral type and age. Astrophys J 902(1):3. https://doi.org/10.3847/1538-4357/abb36f. arXiv:2009.01958 [astro-ph.SR]

Loyd ROP, Shkolnik EL, Schneider AC, et al (2018) HAZMAT. IV. Flares and superflares on young M stars in the far ultraviolet. Astrophys J 867(1):70. https://doi.org/10.3847/1538-4357/aae2ae

Maciel WJ, Costa RDD, Cavichia O (2015) Radial abundance gradients from planetary nebulae at different distances from the galactic plane. Rev Mex Astron Astrofís 51:165. https://doi.org/10.48550/arXiv.1505.07640. arXiv:1505.07640 [astro-ph.GA]

Martin DC, Fanson J, Schiminovich D, et al (2005) The galaxy evolution explorer: a space ultraviolet survey mission. Astrophys J 619(1):L1–L6. https://doi.org/10.1086/426387

Martins F, Schaerer D, Hillier DJ, et al (2005) On stars with weak winds: the galactic case. Astron Astrophys 441(2):735–762. https://doi.org/10.1051/0004-6361:20052927. arXiv:astro-ph/0507278 [astro-ph]

Martins F, Marcolino W, Hillier DJ, et al (2015) Radial dependence of line profile variability in seven O9-B0.5 stars. Astron Astrophys 574:A142. https://doi.org/10.1051/0004-6361/201423882. arXiv:1409.5057 [astro-ph.SR]

Massa D, Fullerton AW, Sonneborn G, et al (2003) Constraints on the ionization balance of hot-star winds from FUSE observations of O stars in the Large Magellanic Cloud. Astrophys J 586(2):996–1018. https://doi.org/10.1086/367786. arXiv:astro-ph/0211518 [astro-ph]

Milone AP, Piotto G, Renzini A, et al (2017) The Hubble Space Telescope UV legacy survey of galactic globular clusters - IX. The atlas of multiple stellar populations. Mon Not R Astron Soc 464(3):3636–3656. https://doi.org/10.1093/mnras/stw2531. arXiv:1610.00451 [astro-ph.SR]

Milone AP, Marino AF, Di Criscienzo M, et al (2018) Multiple stellar populations in Magellanic Cloud clusters - VI. A survey of multiple sequences and Be stars in young clusters. Mon Not R Astron Soc 477(2):2640–2663. https://doi.org/10.1093/mnras/sty661. arXiv:1802.10538 [astro-ph.SR]

Miszalski B, Parker QA, Acker A, et al (2008) MASH-II: more planetary nebulae from the AAO/UKST Hα survey. Mon Not R Astron Soc 384(2):525–534. https://doi.org/10.1111/j.1365-2966.2007.12727.x. arXiv:0711.2923 [astro-ph]

Moos HW, Cash WC, Cowie LL, et al (2000) Overview of the far ultraviolet spectroscopic explorer mission. Astrophys J 538(1):L1–L6. https://doi.org/10.1086/312795

Morton DC (1967) Mass loss from three OB supergiants in Orion. Astrophys J 150:535. https://doi.org/10.1086/149356

Muslimov E, Neiner C (2022) Spectropolarimeter's optical design for the Arago space mission project. arXiv e-prints arXiv:2211.09931. https://doi.org/10.48550/arXiv.2211.09931

Namekata K, Toriumi S, Airapetian VS, et al (2023) Reconstructing the XUV spectra of active sun-like stars using solar scaling relations with magnetic flux. Astrophys J 945(2):147. https://doi.org/10.3847/1538-4357/acbe38

Nardiello D, Libralato M, Piotto G, et al (2018) The Hubble Space Telescope UV legacy survey of galactic globular clusters - XVII. Public catalogue release. Mon Not R Astron Soc 481(3):3382–3393. https://doi.org/10.1093/mnras/sty2515. arXiv:1809.04300 [astro-ph.SR]

National Academies of Sciences, Engineering, and Medicine (2023) Pathways to discovery in astronomy and astrophysics for the 2020s. National Academies Press, Washington. https://doi.org/10.17226/26141

Neiner C, Lapeyrere V, Pechevis E, et al (2025) CASSTOR: a scientific and technology nanosatellite demonstrator for UV spectropolarimetry. arXiv e-prints arXiv:2507.03956. https://doi.org/10.48550/arXiv.2507.03956. arXiv:2507.03956 [astro-ph.IM]

Neiner C, Bouret JC, Fossati L, et al (2026) The Pollux European instrument concept for HWO: a high-resolution spectrograph and spectropolarimeter from the far-UV to the near-IR. arXiv e-prints arXiv:2602.09828. https://doi.org/10.48550/arXiv.2602.09828

Niederhofer F, Georgy C, Bastian N, et al (2015) Apparent age spreads in clusters and the role of stellar rotation. Mon Not R Astron Soc 453(2):2070–2074. https://doi.org/10.1093/mnras/stv1791. arXiv:1507.07561 [astro-ph.SR]

Nieva MF, Przybilla N (2012) Present-day cosmic abundances. A comprehensive study of nearby early B-type stars and implications for stellar and Galactic evolution and interstellar dust models. Astron Astrophys 539:A143. https://doi.org/10.1051/0004-6361/201118158. arXiv:1203.5787 [astro-ph.SR]

Noll S, Kausch W, Barden M, et al (2012) An atmospheric radiation model for Cerro Paranal. I. The optical spectral range. Astron Astrophys 543:A92. https://doi.org/10.1051/0004-6361/201219040. arXiv:1205.2003 [astro-ph.IM]

Noyes RW, Hartmann LW, Baliunas SL, et al (1984) Rotation, convection, and magnetic activity in lower main-sequence stars. Astrophys J 279:763–777. https://doi.org/10.1086/161945

Ohl RG, Chayer P, Moos HW (2000) Photospheric metals in the far ultraviolet spectroscopic explorer spectrum of the subdwarf B star PG 0749+658. Astrophys J 538(1):L95–L98. https://doi.org/10.1086/312802

Osterbrock DE, Ferland GJ (2006) Astrophysics of gaseous nebulae and active galactic nuclei. University Science Books, Sausalito

O'Toole SJ, Heber U (2006) Abundance studies of sdB stars using UV echelle HST/STIS spectroscopy. Astron Astrophys 452(2):579–590. https://doi.org/10.1051/0004-6361:20053948. arXiv:astro-ph/0603069 [astro-ph]
Padovani P, Cirasuolo M (2023) The Extremely Large Telescope. Contemp Phys 64(1):47–64. https://doi.org/10.1080/00107514.2023.2266921. arXiv:2312.04299 [astro-ph.IM]
Parker QA (2022) Planetary nebulae and how to find them: a concise review. Front Astron Space Sci 9:895287. https://doi.org/10.3389/fspas.2022.895287
Parker QA, Phillipps S, Pierce MJ, et al (2005) The AAO/UKST SuperCOSMOS Hα survey. Mon Not R Astron Soc 362(2):689–710. https://doi.org/10.1111/j.1365-2966.2005.09350.x. arXiv:astro-ph/0506599 [astro-ph]
Parker QA, Acker A, Frew DJ, et al (2006) The Macquarie/AAO/Strasbourg Hα planetary nebula catalogue: MASH. Mon Not R Astron Soc 373(1):79–94. https://doi.org/10.1111/j.1365-2966.2006.10950.x
Parker QA, Bojičić IS, Frew DJ (2016) HASH: the Hong Kong/AAO/Strasbourg Hα planetary nebula database. J Phys Conf Ser 728:032008. https://doi.org/10.1088/1742-6596/728/3/032008. arXiv:1603.07042 [astro-ph.SR]
Pineda JS, Youngblood A, France K (2021) The far ultraviolet M-dwarf evolution survey. I. The rotational evolution of high-energy emissions. Astrophys J 911(2):111. https://doi.org/10.3847/1538-4357/abe8d7
Piotto G, Milone AP, Bedin LR, et al (2015) The Hubble Space Telescope UV legacy survey of galactic globular clusters. I. Overview of the project and detection of multiple stellar populations. Astron J 149(3):91. https://doi.org/10.1088/0004-6256/149/3/91. arXiv:1410.4564 [astro-ph.SR]
Pottasch SR (1963) The lower solar corona: interpretation of the ultraviolet spectrum. Astrophys J 137:945–+. https://doi.org/10.1086/147569
Puls J, Vink JS, Najarro F (2008) Mass loss from hot massive stars. Astron Astrophys Rev 16(3–4):209–325. https://doi.org/10.1007/s00159-008-0015-8. arXiv:0811.0487 [astro-ph]
Rao KK, Vaidya K, Agarwal M, et al (2022) Characterization of hot populations of Melotte 66 open cluster using Swift/UVOT. Mon Not R Astron Soc 516(2):2444–2454. https://doi.org/10.1093/mnras/stac2241. arXiv:2208.06659 [astro-ph.GA]
Rauch T, Strauß P (2025) Spectral analysis of HD 49798, a bright, hydrogen-deficient sdO-type donor star in an accreting X-ray binary. Astron Astrophys 700:A80. https://doi.org/10.1051/0004-6361/202555181. arXiv:2507.12912 [astro-ph.SR]
Reid WA, Parker QA (2006) A new population of planetary nebulae discovered in the Large Magellanic Cloud - II. Complete PN catalogue. Mon Not R Astron Soc 373(2):521–550. https://doi.org/10.1111/j.1365-2966.2006.11087.x. arXiv:astro-ph/0610152 [astro-ph]
Reid WA, Parker QA (2013) A new population of planetary nebulae discovered in the Large Magellanic Cloud (IV): the outer LMC. Mon Not R Astron Soc 436(1):604–624. https://doi.org/10.1093/mnras/stt1609. arXiv:1308.5484 [astro-ph.GA]
Roman-Duval J, Fischer WJ, Fullerton AW, et al (2025) The UV Legacy Library of Young Stars as Essential Standards (ULLYSES) large director's discretionary program with Hubble. I. Goals, design, and initial results. Astrophys J 985(1):109. https://doi.org/10.3847/1538-4357/adc45b. arXiv:2504.05446 [astro-ph.SR]
Roming PWA, Kennedy TE, Mason KO, et al (2005) The Swift ultra-violet/optical telescope. Space Sci Rev 120(3–4):95–142. https://doi.org/10.1007/s11214-005-5095-4. arXiv:astro-ph/0507413 [astro-ph]
Rutten RJ (2021) Compendium solar spectrum formation. arXiv e-prints arXiv:2103.02369. https://doi.org/10.48550/arXiv.2103.02369
Rybicki GB, Hummer DG (1992) An accelerated lambda iteration method for multilevel radiative transfer. II. Overlapping transitions with full continuum. Astron Astrophys 262:209–215
Sabin L, Wade GA, Lèbre A (2015) First detection of surface magnetic fields in post-AGB stars: the cases of U Monocerotis and R Scuti. Mon Not R Astron Soc 446(2):1988–1997. https://doi.org/10.1093/mnras/stu2227. arXiv:1410.6224 [astro-ph.SR]
Sandlin GD, Bartoe JDF, Brueckner GE, et al (1986) The high-resolution solar spectrum, 1175-1710 Å. Astrophys J Suppl Ser 61:801–898
Sbordone L, Salaris M, Weiss A, et al (2011) Photometric signatures of multiple stellar populations in Galactic globular clusters. Astron Astrophys 534:A9. https://doi.org/10.1051/0004-6361/201116714. arXiv:1103.5863 [astro-ph.SR]
Scowen PA, Gayley K, Ignace R, et al (2022) The Polstar high resolution spectropolarimetry MIDEX mission. Astrophys Space Sci 367(12):121. https://doi.org/10.1007/s10509-022-04107-9. arXiv:2108.10729 [astro-ph.IM]
Seaton MJ (1987) Atomic data for opacity calculations. I. General description. J Phys B 20(23):6363–6378. https://doi.org/10.1088/0022-3700/20/23/026
Seli B, Oláh K, Kriskovics L, et al (2022) Extending the FIP bias sample to magnetically active stars. Challenging the FIP bias paradigm. Astron Astrophys 659:A3. https://doi.org/10.1051/0004-6361/202141493

Shvartzvald Y, Waxman E, Gal-Yam A, et al (2024) ULTRASAT: a wide-field time-domain UV space telescope. Astrophys J 964(1):74. https://doi.org/10.3847/1538-4357/ad2704. arXiv:2304.14482 [astro-ph.IM]
Sim SA, Jordan C (2005) Modelling the chromosphere and transition region of ϵ Eri (K2 V). Mon Not R Astron Soc 361:1102–1120. https://doi.org/10.1111/j.1365-2966.2005.09247.x
Sindhu N, Subramaniam A, Jadhav VV, et al (2019) UVIT open cluster study. I. detection of a white dwarf companion to a blue straggler in M67: evidence of formation through mass transfer. Astrophys J 882(1):43. https://doi.org/10.3847/1538-4357/ab31a8. arXiv:1907.05556 [astro-ph.SR]
Smith CL, Zijlstra AA, Gesicki KM, et al (2017) Abundances in Galactic bulge planetary nebulae from optical, ultraviolet and infrared observations. Mon Not R Astron Soc 471(3):3008–3018. https://doi.org/10.1093/mnras/stx1720. arXiv:1707.06672 [astro-ph.SR]
Stanford SA, Murison MA, Whitney BA, et al (1985) The Wisconsin ultraviolet photo-polarimeter experiment. In: Bulletin of the American Astronomical Society, p 900
Stanghellini L, Haywood M (2018) Galactic planetary nebulae as probes of radial metallicity gradients and other abundance patterns. Astrophys J 862(1):45. https://doi.org/10.3847/1538-4357/aacaf8. arXiv:1806.02276 [astro-ph.GA]
Storey PJ (1981) Dielectronic recombination at nebular temperatures. Mon Not R Astron Soc 195:27P–31. https://doi.org/10.1093/mnras/195.1.27P
Storey PJ, Hummer DG (1995) Recombination line intensities for hydrogenic ions-IV. Total recombination coefficients and machine-readable tables for Z = 1 to 8. Mon Not R Astron Soc 272(1):41–48. https://doi.org/10.1093/mnras/272.1.41
Storey PJ, Dufresne RP, Del Zanna G (2023) New atomic data for C I Rydberg states compared with solar UV spectra. Mon Not R Astron Soc 526(1):1396–1407. https://doi.org/10.1093/mnras/stad2736
Subramaniam A, Sindhu N, Tandon SN, et al (2016) A hot companion to a blue straggler in NGC 188 as revealed by the Ultra-Violet Imaging Telescope (UVIT) on ASTROSAT. Astrophys J 833(2):L27. https://doi.org/10.3847/2041-8213/833/2/L27
Summers HP (1974) The ionization equilibrium of hydrogen-like to argon-like ions of elements. Mon Not R Astron Soc 169:663–680
Sun W, Li C, Deng L, et al (2019) Tidal-locking-induced stellar rotation dichotomy in the open cluster NGC 2287? Astrophys J 883(2):182. https://doi.org/10.3847/1538-4357/ab3cd0. arXiv:1908.06530 [astro-ph.SR]
Sundqvist JO, Owocki SP (2013) Clumping in the inner winds of hot, massive stars from hydrodynamical line-driven instability simulations. Mon Not R Astron Soc 428(2):1837–1844. https://doi.org/10.1093/mnras/sts165. arXiv:1210.1861 [astro-ph.SR]
Tan S, Parker QA, Zijlstra AA, et al (2024) A catalogue of planetary nebulae chemical abundances in the Galactic bulge. Mon Not R Astron Soc 527(3):6363–6387. https://doi.org/10.1093/mnras/stad3496. arXiv:2311.01836 [astro-ph.GA]
Tessore B, Pinte C, Bouvier J, et al (2021) Atomic line radiative transfer with MCFOST. I. Code description and benchmarking. Astron Astrophys 647:A27. https://doi.org/10.1051/0004-6361/202039697
Thaller ML, Bagnuolo WG Jr, Gies DR, et al (1995) Tomographic Separation of Composite Spectra. III. Ultraviolet Detection of the Hot Companion of phi Persei. Astrophys J 448:878. https://doi.org/10.1086/176016
The LUVOIR Team (2019) The LUVOIR mission concept study final report. arXiv:1912.06219
Tumlinson J, Peeples MS, Werk JK (2017) The circumgalactic medium. Annu Rev Astron Astrophys 55(1):389–432. https://doi.org/10.1146/annurev-astro-091916-055240. arXiv:1709.09180 [astro-ph.GA]
Uitenbroek H (2001) Multilevel radiative transfer with partial frequency redistribution. Astrophys J 557(1):389–398. https://doi.org/10.1086/321659
van Duinen RJ, Aalders JWG, Wesselius PR, et al (1975) The ultraviolet experiment onboard the Astronomical Netherlands Satellite - ANS. Astron Astrophys 39:159–163
van Velzen S, Gezari S, Hammerstein E, et al (2021) Seventeen tidal disruption events from the first half of ZTF survey observations: entering a new era of population studies. Astrophys J 908(1):4. https://doi.org/10.3847/1538-4357/abc258. arXiv:2001.01409 [astro-ph.HE]
Vennes S, Kawka A, Németh P (2011) A selection of hot subluminous stars in the GALEX survey - I. Correlation with the Guide Star Catalog. Mon Not R Astron Soc 410(3):2095–2112. https://doi.org/10.1111/j.1365-2966.2010.17584.x. arXiv:1008.3823 [astro-ph.SR]
Vernazza JE, Avrett EH, Loeser R (1973) Structure of the solar chromosphere. Basic computations and summary of the results. Astrophys J 184:605–632. https://doi.org/10.1086/152353
Vink JS, de Koter A, Lamers HJGLM (2001) Mass-loss predictions for O and B stars as a function of metallicity. Astron Astrophys 369:574–588. https://doi.org/10.1051/0004-6361:20010127. arXiv:astro-ph/0101509 [astro-ph]

Vink JS, Mehner A, Crowther PA, et al (2023) X-Shooting ULLYSES: massive stars at low metallicity. I. Project description. Astron Astrophys 675:A154. https://doi.org/10.1051/0004-6361/202245650. arXiv:2305.06376 [astro-ph.SR]
Viton M, Burgarella D, Cassatella A, et al (1988) The Spacelab-1 very wide field survey of UV-excess objects. I. CPD -71 172 AB, a new binary with a hot subdwarf. Astron Astrophys 205:147–154
Walborn NR, Panek RJ (1984) Ultraviolet spectral morphology of the O stars. II. The main sequence. Astrophys J 280:155–162. https://doi.org/10.1086/162013
Werner K (1996) On the Balmer line problem. Astrophys J 457:L39. https://doi.org/10.1086/309889
Wesemael F, Holberg JB, Veilleux S, et al (1985) Studies of hot B subdwarfs. II. Energy distributions of three bright sdB/sdOB stars in the 950-5500 A range. Astrophys J 298:859–866. https://doi.org/10.1086/163669
Wesselius PR, Aalders JWG, van Albada TS, et al (1976) Preliminary results obtained with the UV spectrophotometer, onboard ANS. In: Kharadze EK (ed) Stars and galaxies from observational points of view, pp 67–74
Windhorst RA, Cohen SH, Jansen RA, et al (2023) JWST PEARLS. Prime extragalactic areas for reionization and lensing science: project overview and first results. Astron J 165(1):13. https://doi.org/10.3847/1538-3881/aca163. arXiv:2209.04119 [astro-ph.CO]
Wood BE, Linsky JL (2010) Resolving the ξ Boo binary with Chandra, and revealing the spectral type dependence of the coronal "FIP effect". Astrophys J 717(2):1279–1290. https://doi.org/10.1088/0004-637X/717/2/1279
Woodgate BE, Kimble RA, Bowers CW, et al (1998) The space telescope imaging spectrograph design. Publ Astron Soc Pac 110(752):1183–1204. https://doi.org/10.1086/316243
Zhang CY, Badnell NR, Storey PJ, et al (2025) Dielectronic recombination of iron M-shell ions: Fe8+ and Fe7+. Mon Not R Astron Soc 543(1):314–325. https://doi.org/10.1093/mnras/staf1456

Publisher's Note Springer Nature remains neutral with regard to jurisdictional claims in published maps and institutional affiliations.

Authors and Affiliations

Xiaoting Fu[1] · Giulio Del Zanna[2,3] · Li Ji[1] · Stephan Geier[4] · Matti Dorsch[4] · Vikrant Jadhav[5,6] · Firoza Sutaria[7] · Chengyuan Li[8,9] · Quentin Parker[10] · Xuan Fang[11,12]

✉ G. Del Zanna
gd232@cam.ac.uk

1 Purple Mountain Observatory, Chinese Academy of Sciences, Yuanhua road 10, Nanjing, 210023, China

2 DAMTP, University of Cambridge, Wilberforce Road, Cambridge, CB3 0WA, UK

3 School of Physics & Astronomy, University of Leicester, Leicester, LE1 7RH, UK

4 Institute for Physics and Astronomy, University of Potsdam, Karl-Liebknecht-Str. 24/25, Potsdam, 14467, Germany

5 Astronomical Institute, Faculty of Mathematics and Physics, Charles University, V Holešovičkách 2, Praha, 18000, Czech Republic

6 Helmholtz Institute for Radiation and Nuclear Physics, University of Bonn, Nussallee 14-15, Bonn, 53115, Germany

7 Indian Institute of Astrophysics, Koramangala, Block II, Bangalore, 560034, India

8 School of Physics and Astronomy, Sun Yat-sen University, Daxue Road, Zhuhai, Guangdong 519082, China

9 CSST Science Center for the Guangdong-Hong Kong-Macau Greater Bay Area, Zhuhai 519082, China

[10] Laboratory for Space Research, University of Hong Kong, Cyberport 4, PokFuLam, Hong Kong SAR, P.R. China

[11] National Astronomical Observatories, Chinese Academy of Sciences (NAOC), 20 A Datun road, Beijing, 100101, China

[12] School of Astronomy and Space Sciences, University of Chinese Academy of Science (UCAS), Beijing, 100049, China